High Power Millimeter Wave Gyrotron

Jianxun Wang

Microwave/Millimeter Wave Technology Enginer Center

Dept of Physical Electronics

University of Electronic Science and Technology, Cheng Du, China

Outline

- Gyrotron Introduction
- Electron Gun for Gyrotron
- Cavities of Gyrotron
- The design of a Gyroklystron

Gyrotron Introduction

The Gyrotron: Cyclotron Resonance Maser (CRM)

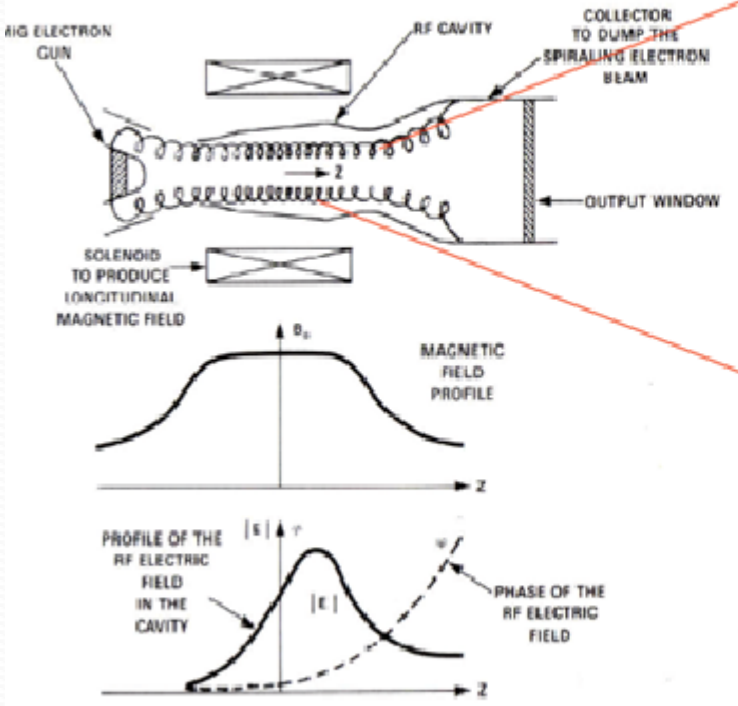

- Magnetized weakly-relativistic electron beam (non-neutral plasma)
- Electron cyclotron frequency:

$$\Omega_c = -eB_0/m_0\gamma_0; \quad \gamma_0 = 1+E_0/m_0c^2$$

- Electron-beam distribution function

$$f_0(p_\perp, p_\parallel) = \frac{1}{2\pi p_{\perp 0}}\delta(p_\perp - p_{\perp 0})\delta(p_\parallel - p_{\parallel 0})$$

f_0 is CRM unstable

- EM cavity resonant at frequency ω_{THz}
- Resonance condition:

$$s\,\Omega_c \approx \omega_{THz}$$

(s,harmonic number)

$f_{THz} = s/\gamma_0$ B 28GHz/T (γ_0 = 1.02-1.04)
(E_0 = 10-20 keV)

- Kinetic rotational (perpendicular) energy efficiently converted into EM waves (max $\eta_{perp} = P_{EM}/P_{rot}$ = 70%)

Extraordinary high average power at millimeter wavelengths
MW power level in oscillators; tens kW in amplifiers

Gyrotron for magnetic fusion application: a/λ ≈ 10-15

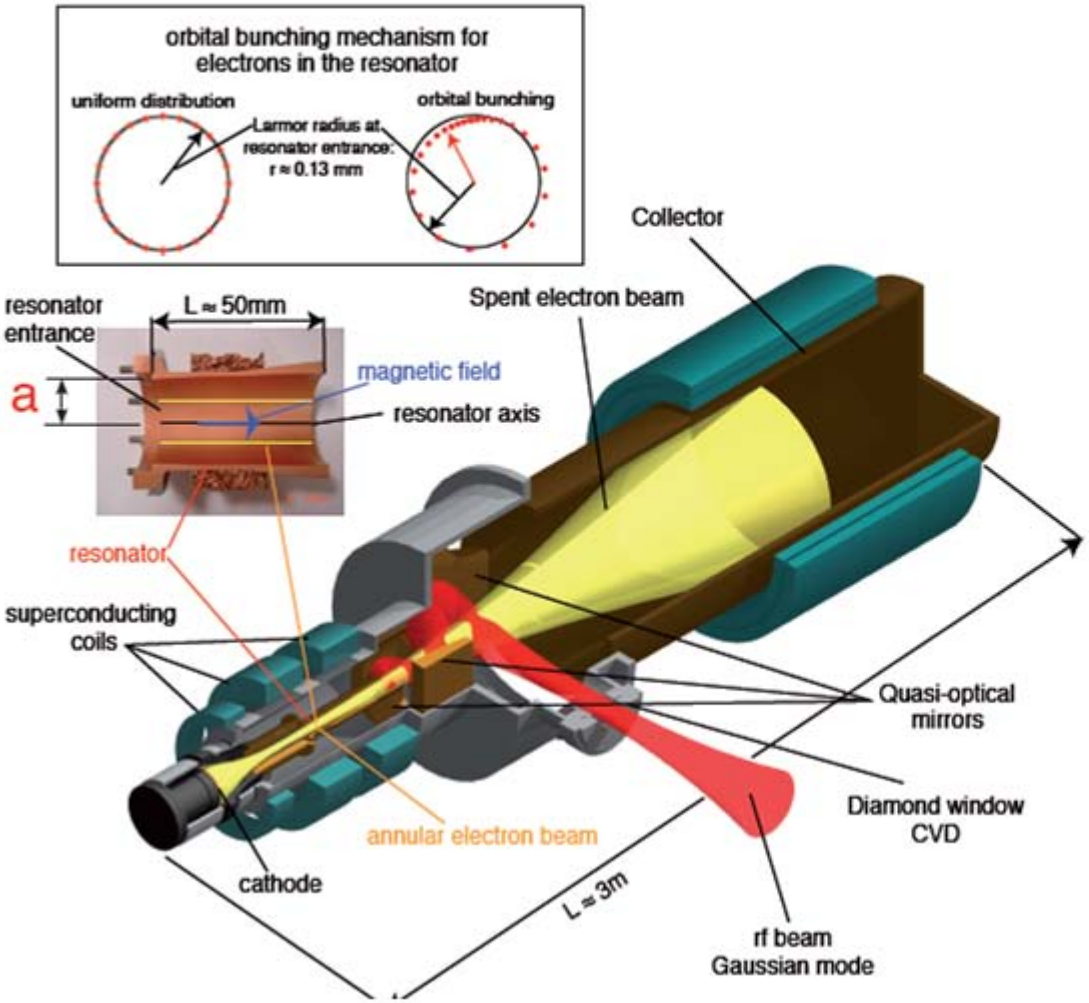

2MW 170GHz Coaxial Gyrotron

Performance Domains for Vacuum (Fast- and Slow-Wave) and Solid-State

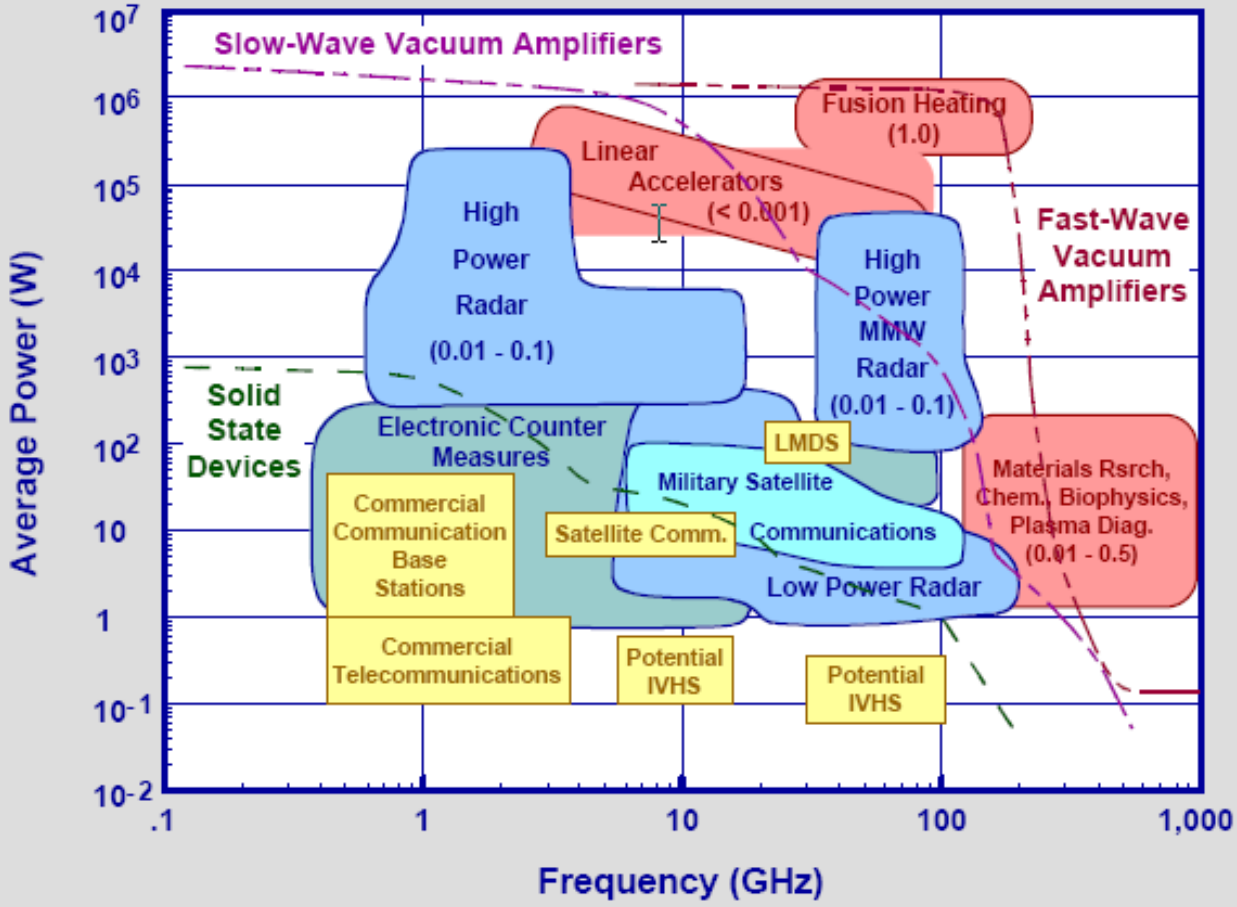

Key to Applications

Military
Commercial
Scientific

Physics
- Mobility
- heat dissipation
- voltages

Gyrotrons (110-170 GHz) for ECRH Systems of Fusion Devices and ITER

Institution	Frequency	Mode		Power	Efficiency	Pulse length	Fusion Device
	[GHz]	cavity	output	[MW]	[%]	[s]	
CPI, Palo Alto	110	$TE_{22,6}$	TEM_{00}	1.05	31	5.0	D III - D
				0.6	31	10.0	"
	140	$TE_{28,7}$	TEM_{00}	0.9	33 (SDC)	1800	W7-X
GYCOM-M (TORIY, IAP) Moscow, N. Novgorod	110	$TE_{19,5}$	TEM_{00}	0.93	36	2.0	D III - D
				0.5	35	5.0	"
				0.35	33	10.0	"
	140	$TE_{22,6}$	TEM_{00}	0.96	36	1.2	ASDEX - U
				0.54	36	3.0	W7 – AS
	170	$TE_{25,10}$	TEM_{00}	0.90	44 (SDC)	21	ITER
				0.50	40 (SDC)	300	"
GYCOM-N (SALUT, IAP) Nizhny Novgorod	140	$TE_{22,6}$	TEM_{00}	0.8	32	0.8	W7 - AS
				0.88	50.5 (SDC)	1.0	"
	158.5	$TE_{24,7}$	TEM_{00}	0.5	30	0.7	T 10
JAEA, TOSHIBA Naka, Otawara	110	$TE_{22,6}$	TEM_{00}	1.2	39 (SDC)	4.1	JT 60 - U
				1.0	39 (SDC)	5.0	"
	170	$TE_{31,8}$	TEM_{00}	0.9	43.4 (SDC)	9.0	ITER
				0.6	46 (SDC)	3600	"
				0.82	56 (SDC)	600	"
THALES, CEA,CRPP, FZK	118	$TE_{22,6}$	TEM_{00}	0.53	32	5.0	TORE SUPRA
				0.35	23	111	"
Europe	140	$TE_{28,8}$	TEM_{00}	1.00	49 (SDC)	12	W7 - X
				0.92	45 (SDC)	1800	"

Present State-of-the-Art of High Power Gyrotrons

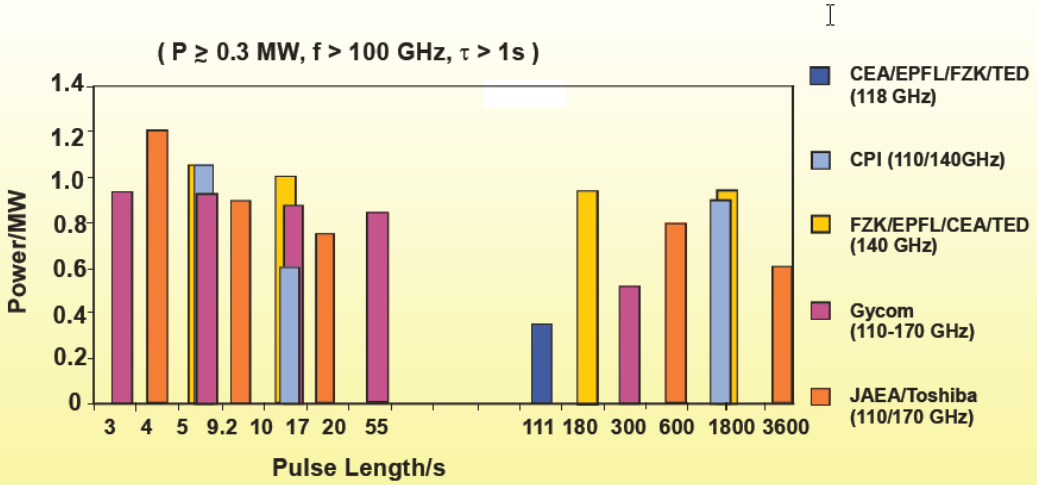

High Frequency Output Coupling for Gyrotrons

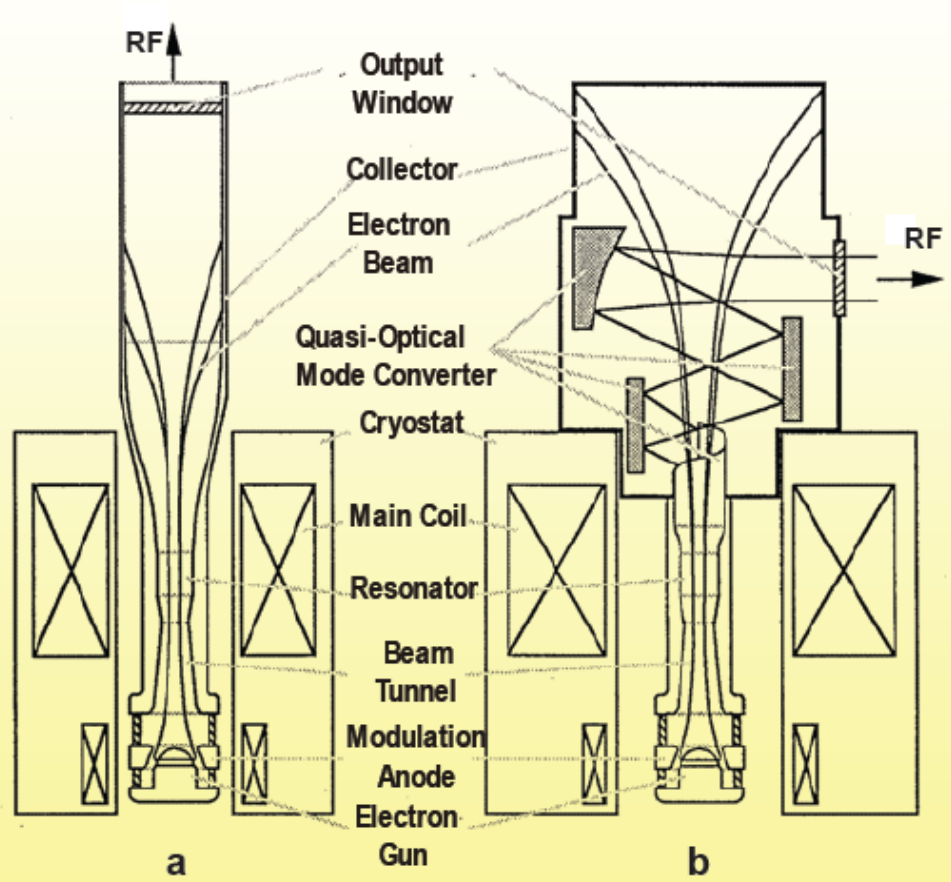

Axial Output Coupling through Oversized Circular Waveguide e.g. TE_{03}

Advantages

- Isolator for Reflections
- Optimum Mode for Transmission
- Free Choice of Collector Design

Radial Output Coupling through Optical Elements TEM_{00} (Gaussian Beam)

Common classes of cavity modes used in gyrotrons

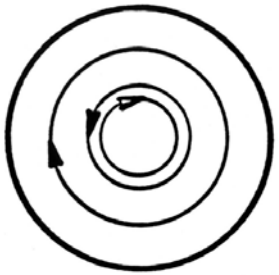

(a) TE_{on} Modes

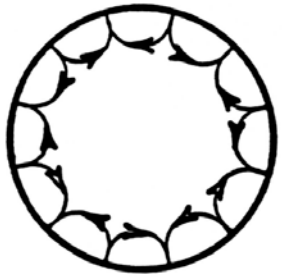

(b) Whispering Gallery Modes

$TE_{m,p}$ $(m >> p)$

(c) TE_{ln} Modes

$TE_{0,2}$

$D/\lambda \approx 2.2$

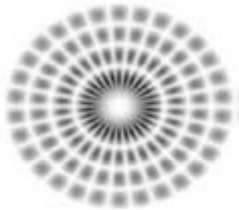

$TE_{15,4}$

$D/\lambda \approx 10$

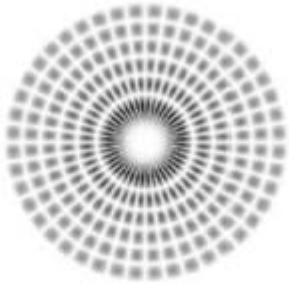

$TE_{22,6}$

$D/\lambda \approx 15$

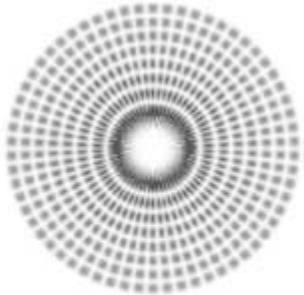

$TE_{31,8}$ or $TE_{25,10}$

$D/\lambda \approx 20$

GYROTRON -expensive, large and heavy device - up to 3m, up to 1000kg

Increasing of Gyrotron operating frequency, power and pulse energy by increasing operating voltage, current and cavity dimensions

The First 30 Modes of Circular Waveguide

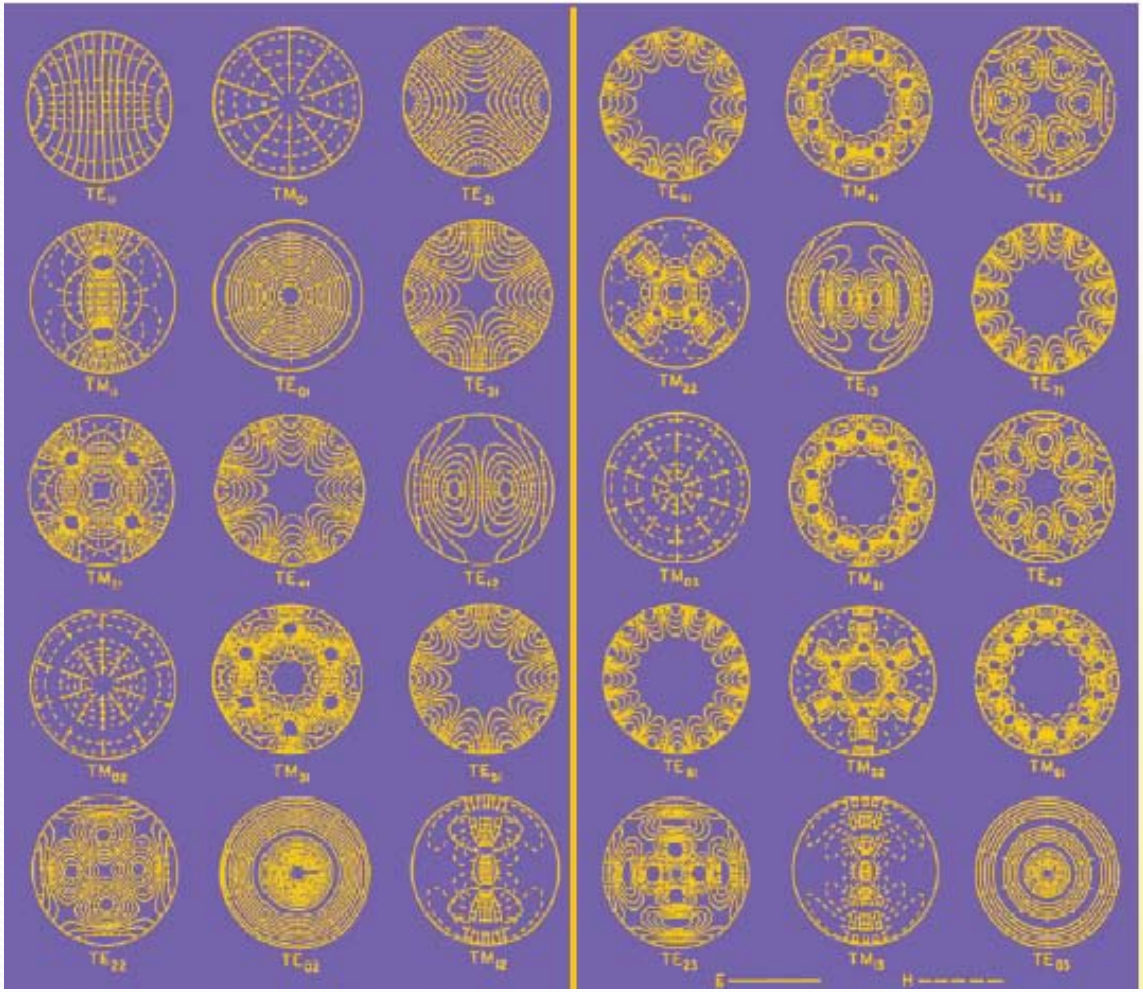

Number of propagating Modes

$$N \approx 2.55 (D/\lambda_0)^2$$

D : Waveguide Diameter

λ_0 : Free Space Wavelength

Gyrotron - Oscillator

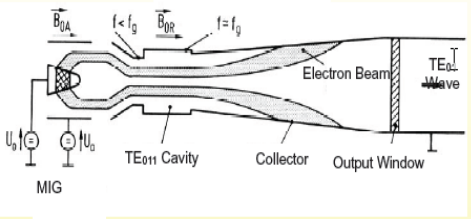

Gyroklstron

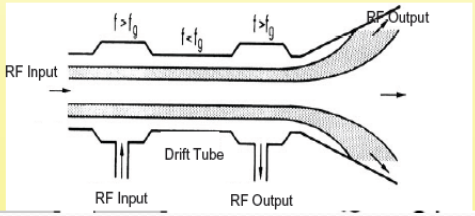

Gyro -Travelling- Wave Tube

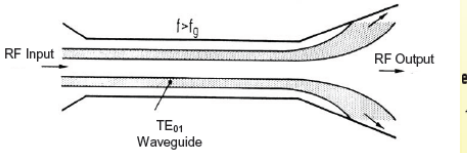

Gyro-BWO

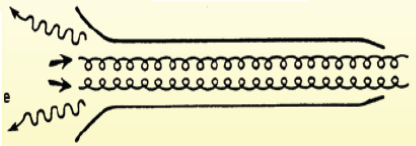

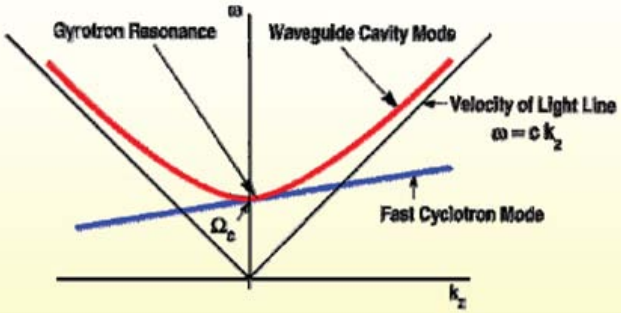

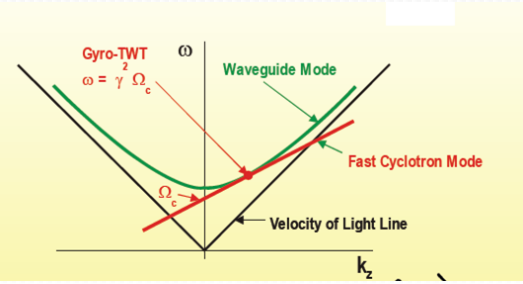

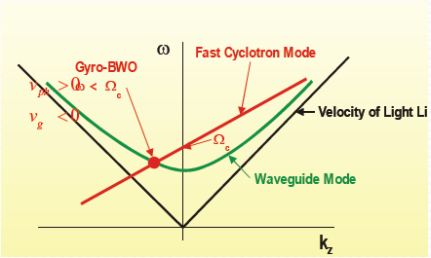

electromagnetic waveguide mode :

$$\omega^2 = (k_z c)^2 + (k_\perp c)^2 \quad \text{(hyperbola)}$$

with $k_\perp = \frac{X'_{mn}}{R_0}$ (X'_{mn} Bessel zero)

beam - wave resonance for $k_\perp >> k_z$:

$\omega \gtrsim s\,\Omega_c$, s = 1, 2,... (straight lines)

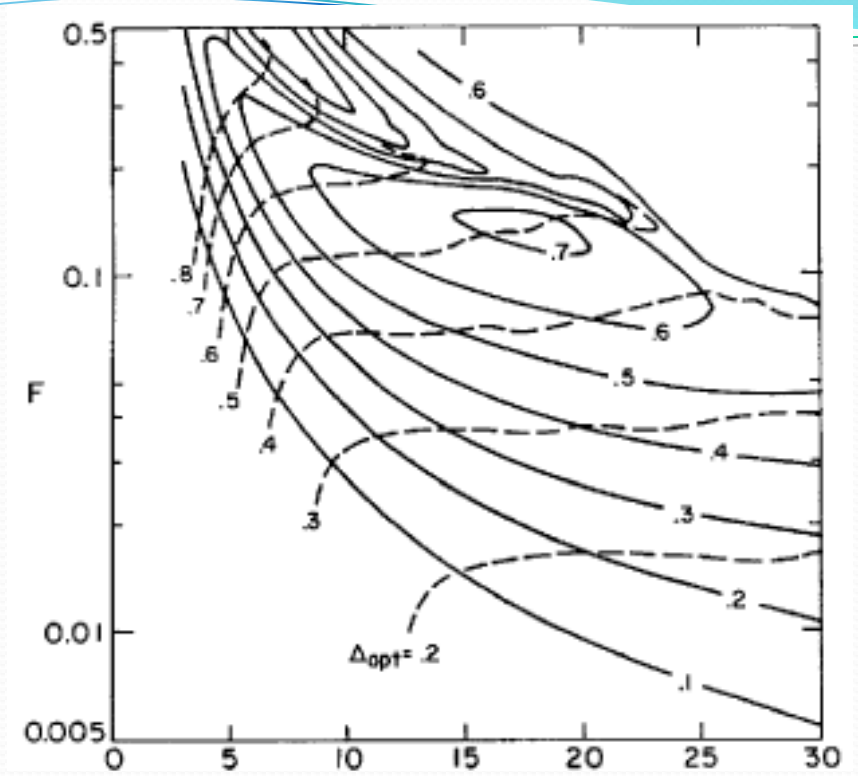

Contour plot of transverse efficiency (solid lines) and optimum magnetic field detuning Δ_{opt} (dashed lines) as a function of normalized field amplitude F and cavity length μ for fundamental gyrotron interaction ($\omega \approx \Omega_c$)

$$\eta_{max} = \frac{\alpha^2}{1+\alpha^2}\eta_{\perp} \qquad \alpha = 1.5, \eta_{max} = 50\%$$

Gyrotrons for Fusion

The main problems of powerful CW gyrotrons of a millimeter range

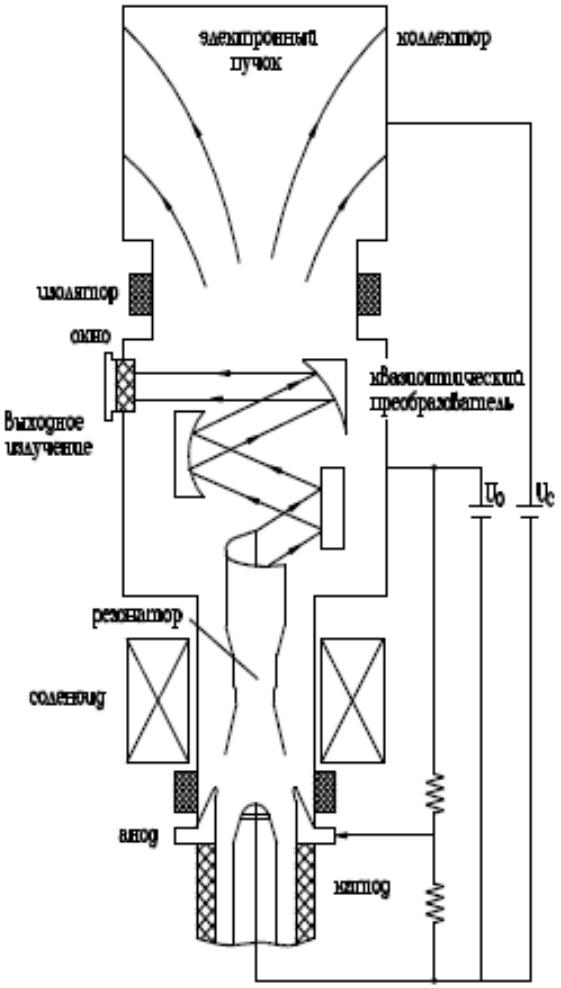

- Formation of intensive helical electron beams (HEB), with large enough oscillatory energy and acceptable velocity spread;
- Maintenance of stable, high efficient generation of an operating mode in oversized cavities;
- Effective conversion of an operating mode to a wave beam, with optimization of its spatial distribution;
- Development of a reliable collector of an electron beam;
- Creation of an output window capable to transmit high-frequency radiation from gyrotron in working regime.

High-Harmonic THz Gyrotron (LO)

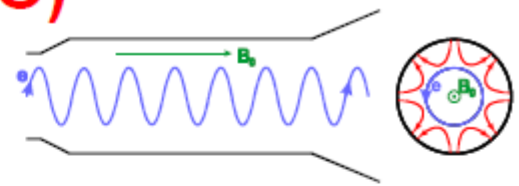

Advantage: s-times lower magnetic field

Problem: mode competition

$$\omega = s\omega_{cyclotron}$$

Large-orbit gyrotron: high-selective geometry (azimuthal mode index = harmonic number)

CW version based on CM is under development

$$G = \frac{J^2_{m-s}(k_\perp R_b)}{(\nu^2_{m,p} - m^2)J^2_m(\nu_{m,p})}$$

$$m \neq s, G = 0 \qquad R_b = 0$$

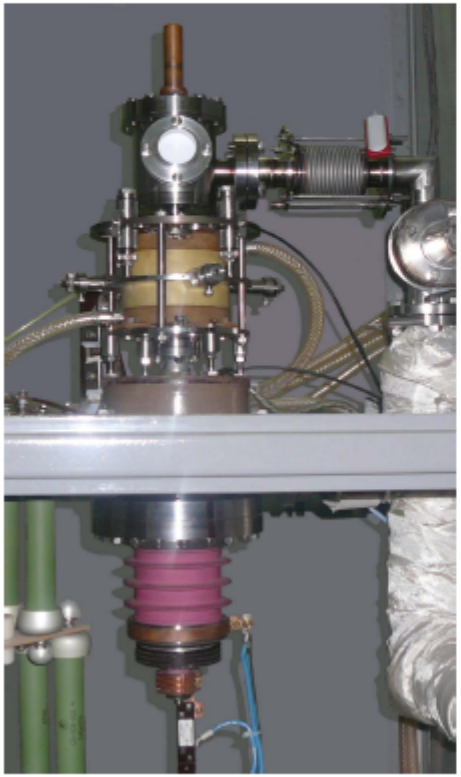

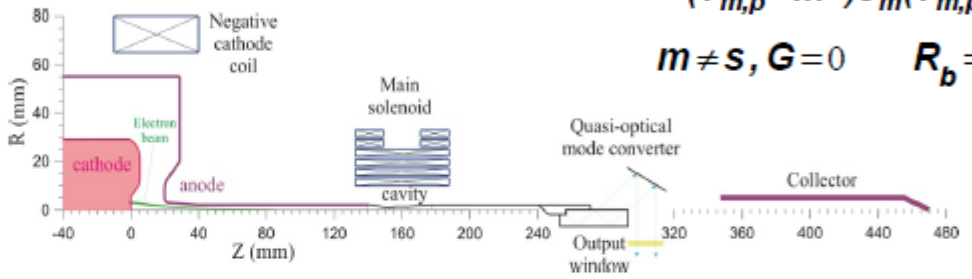

Operating mode	$TE_{2,4}$	$TE_{2,5}$	$TE_{3,6}$	$TE_{3,7}$
Harmonic number, *s*	2	2	3	3
Frequency, THz	0.55	0.68	0.87	1.0
Beam voltage, kV	50	80	60	80
Magnetic field, T	10.6	13.8	11.5	13.6
Efficiency, %	2.2	3.5	0.9	1.5
Output power, kW	0.6	1.8	0.3	0.4

V.L. Bratman, Yu.K. Kalynov, V.N. Manuilov, 2008

Low Voltage Operation

- *Goldenberg, A., Glyavin, M., Zavolsky, N., Manuilo,v V. Technological gyrotron with low*
Radiophysics and Quantum Electronics, Vol. 48, N 10-11, 2005, pp. 741-747
- *M.K.Hornstein, V.S.Bajaj, R. G. Griffin and R. J. Temkin Efficient Low-Voltage Operation*
Oscillator at 233 GHz // IEEE Trans. Plasma Sci., 2007, 35, 1, p.27

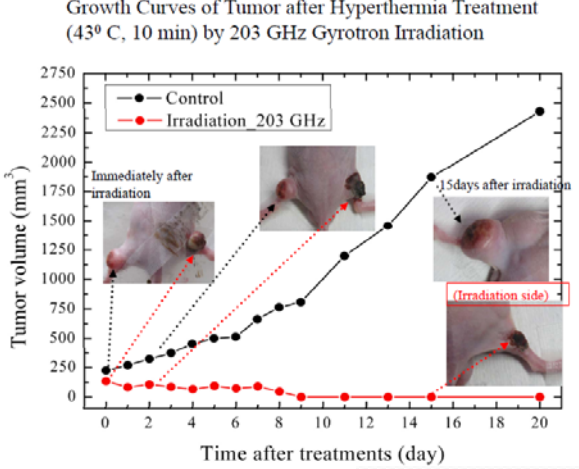

Theoretical investigation of $TE_{2,2}$ mode with frequency f = 203GHz

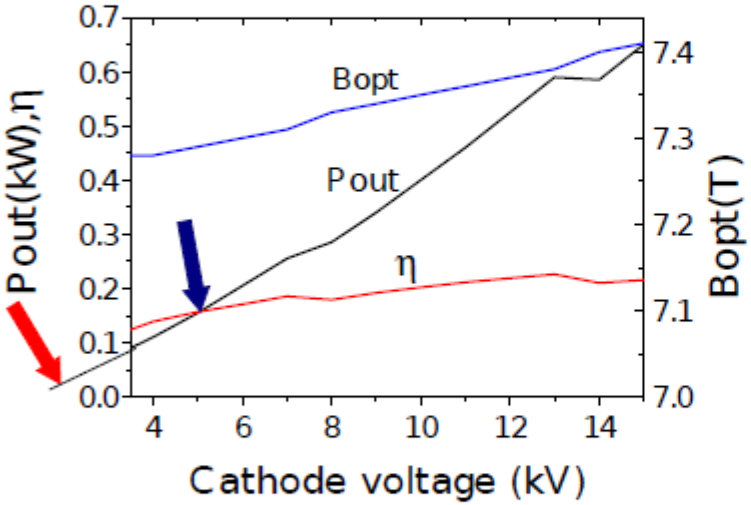

U=2 kV
I_{beam} = 0.5 A
Efficiency ~ 1%
Power ~ 25 W
R_{beam} ~ 1mm

U=5 kV
I_{beam} = 0.2 A
Efficiency ~ 15%
Power ~ 200 W
R_{beam} =0.4 mm

4 NbTi coils, warm bore diameter: 100 mm
Maximal magnetic field : 8.0 T

Gyrotron Electron Beam Formation

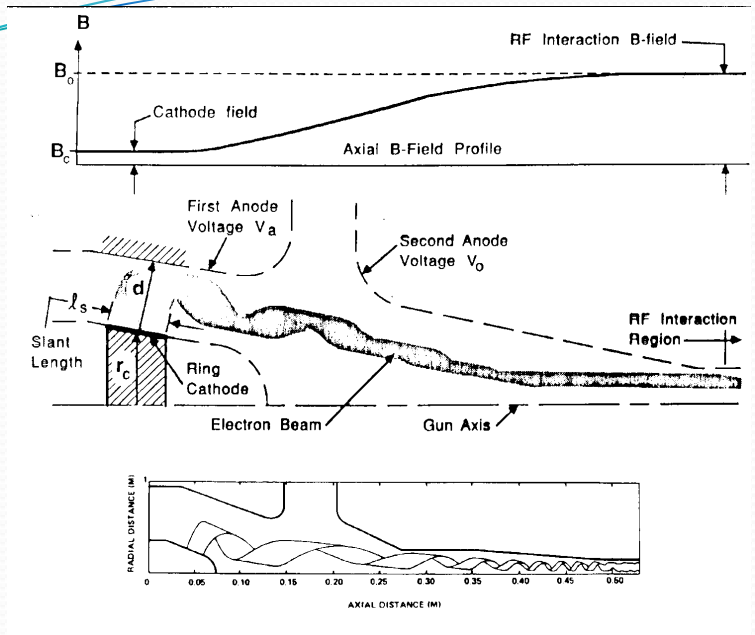

General outline of a magnetron injection gun with two anodes including a plot of a typical magnetic field profile.

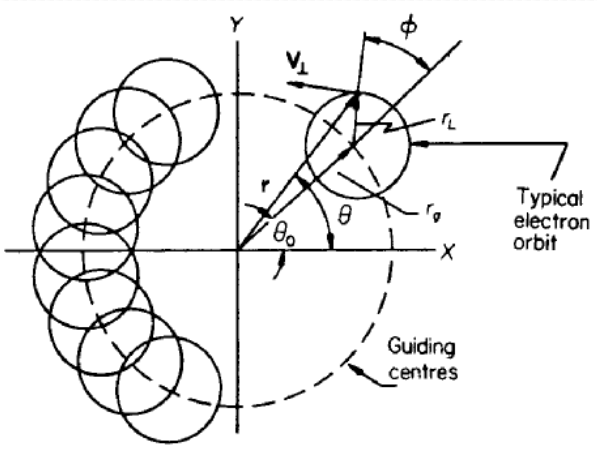

Diagram of beam cross-section after acceleration to final voltage showing the guiding center and Larmor radii.

Gyrotron generally requires an electron beam with $\alpha = v_\perp/v \approx 1.5$. The most common approach to obtaining such a beam is the magnetron injection gun.

The function of the first anode is to provide a region of radial electrical field which serves to impart transverse motion to the electrons which are emitted from the annular ring cathode. Because the magnetic field is primarily axial, the electron motion is in the form of a cycloid which consists of the circular orbital motion superimposed upon the familiar drift.

The presence of the second anode results in an axial electric field which accelerates the electrons toward the direction of increasing magnetic field. As the electrons gain axial velocity, the increasing magnetic field results in a transformation of energy into rotational through the $v_z B_{r|}$ force. The resultant beam at the position of the rf interaction region is therefore of the required form as shown.

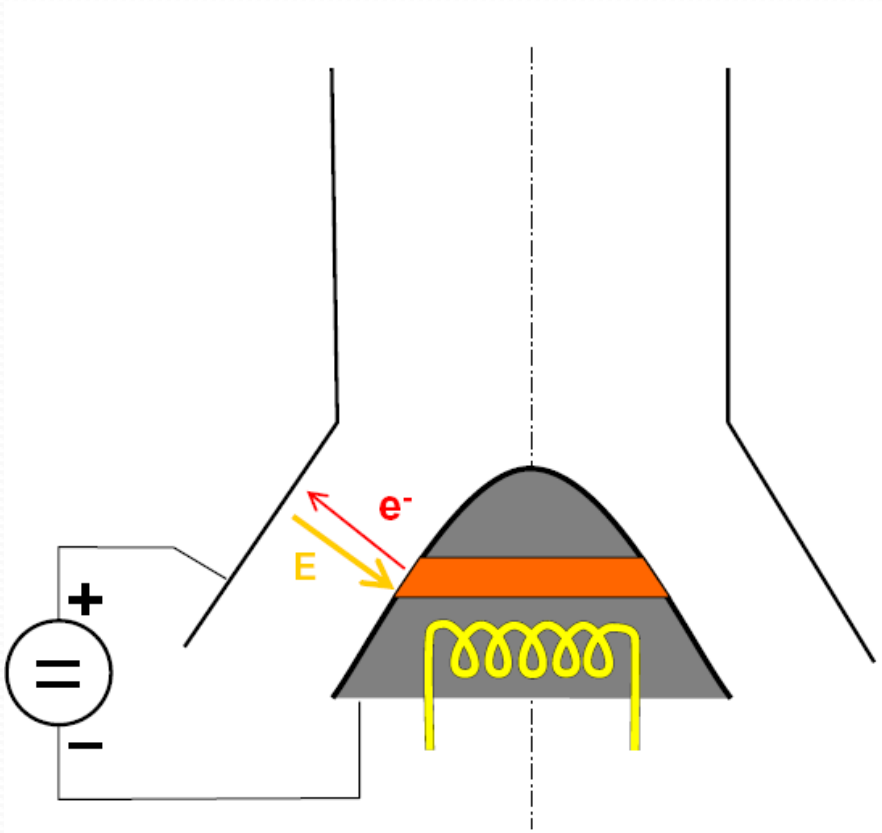

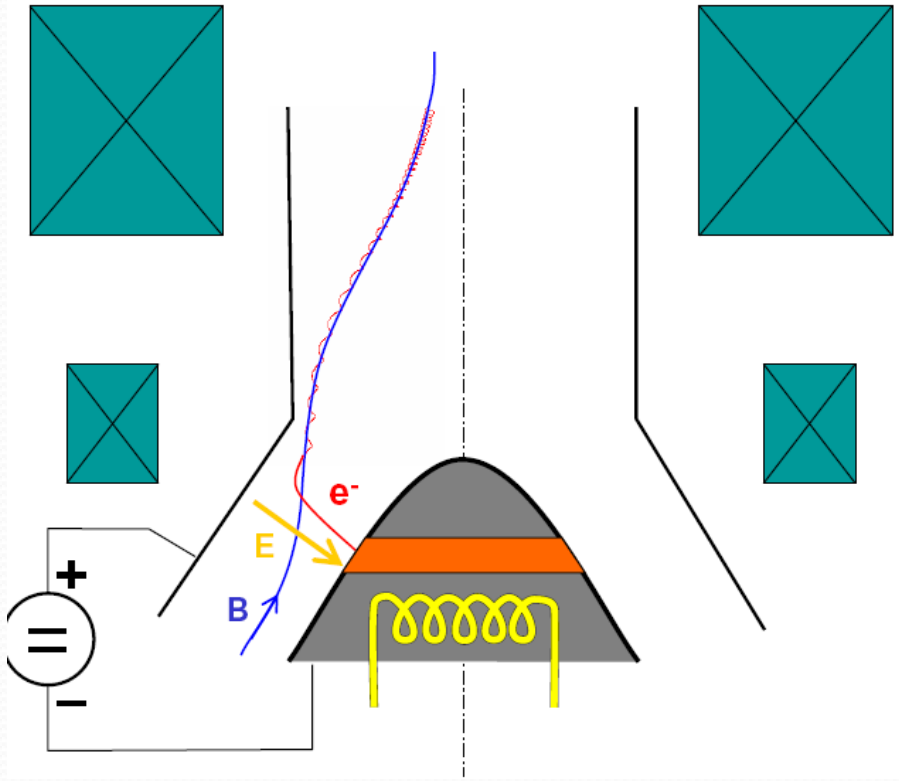

Generation of an Angular Electron Beam

Generation of an Annular Electron Beam

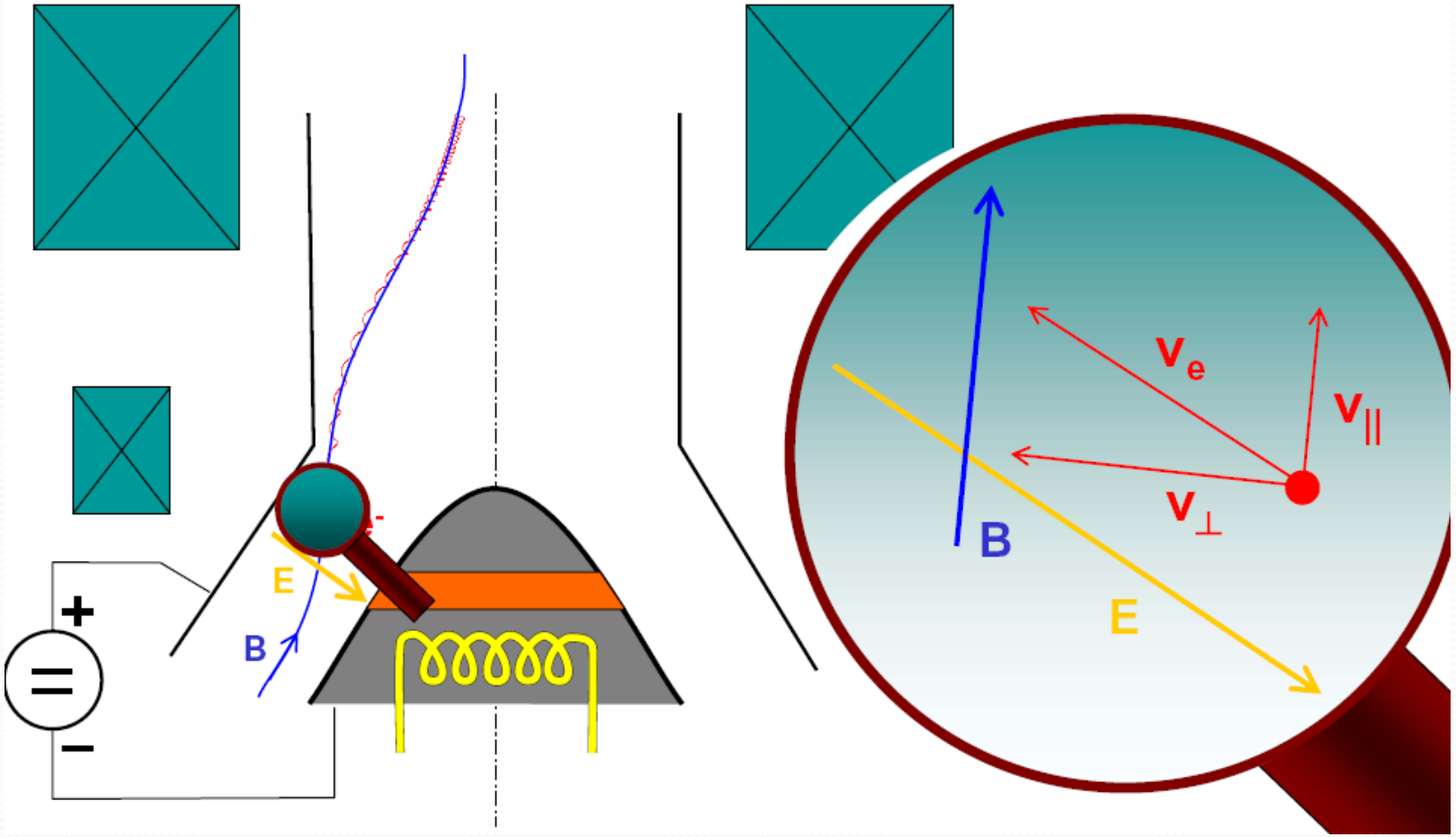

Generation of an Annular Electron Beam

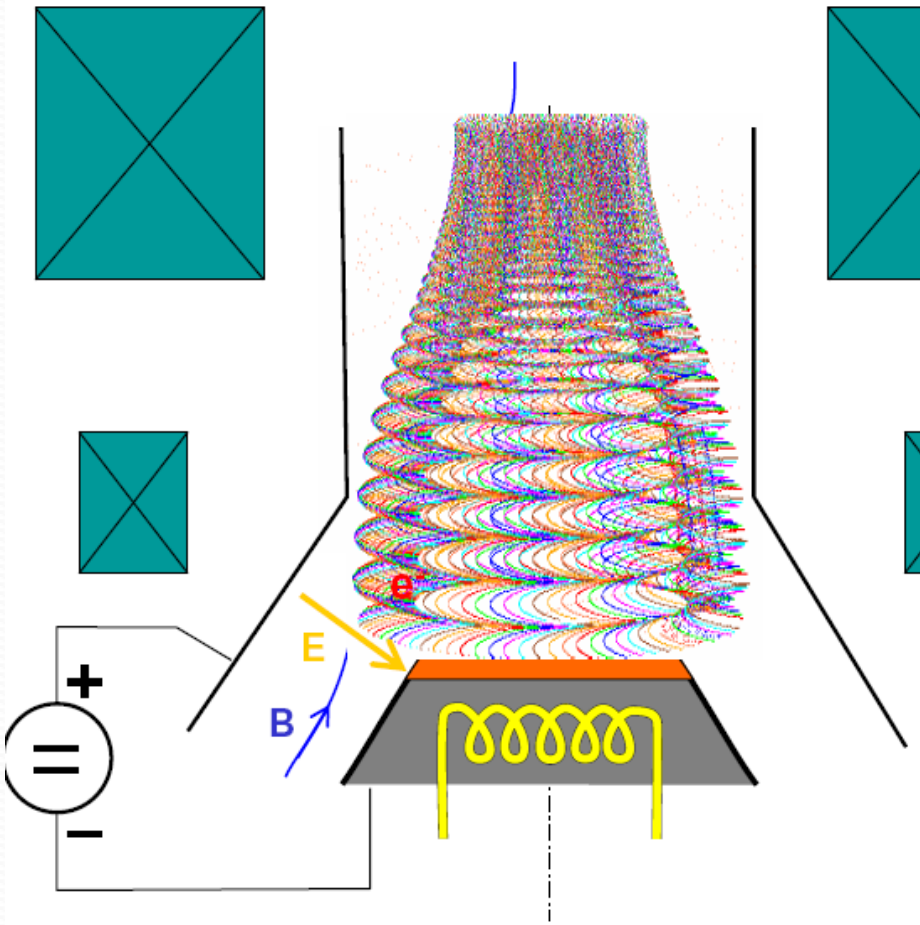

B increases

$v_\perp$ increases

$v_{||}$ decreases

$\alpha = v_\perp / v_{||}$ increases

magnetron injection gun (MIG)

Electron Gun types

Diode gun

Triode gun

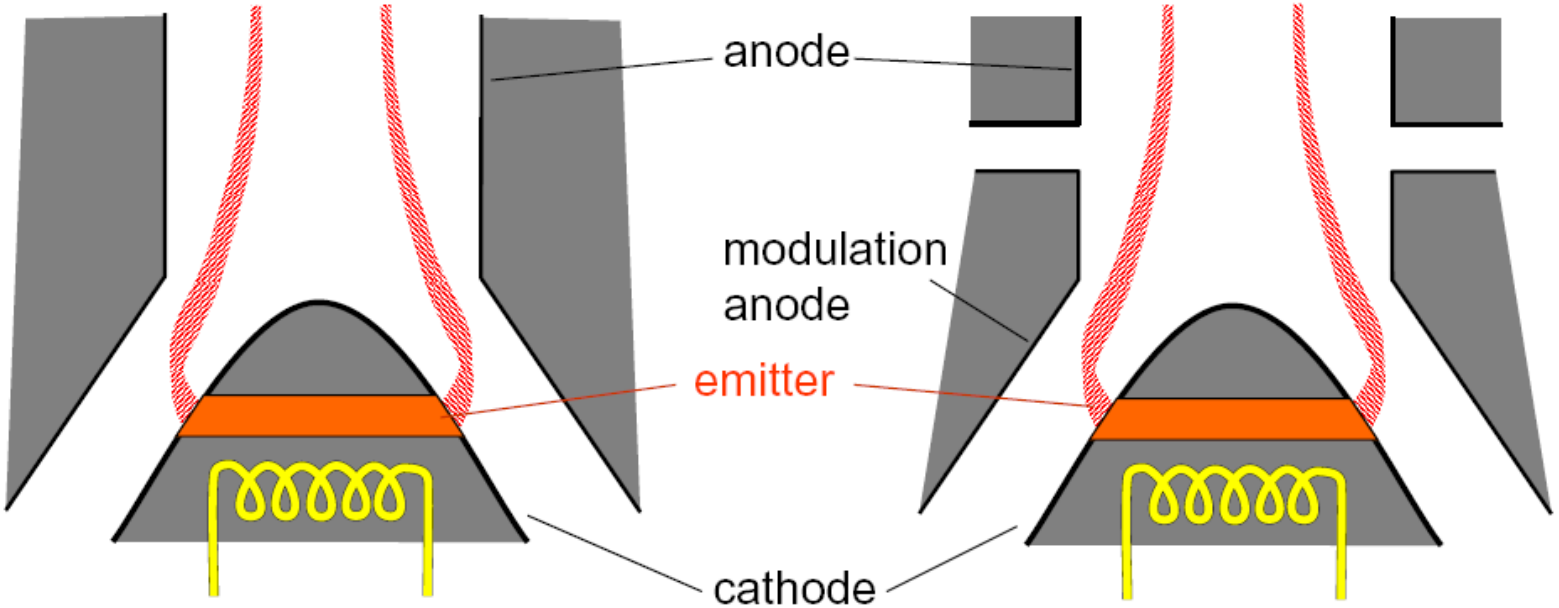

α is a function of the acceleration voltage U_{acc}

more complicated, but independend control over α

Large Magnetic Compression Eases Cathode Loading

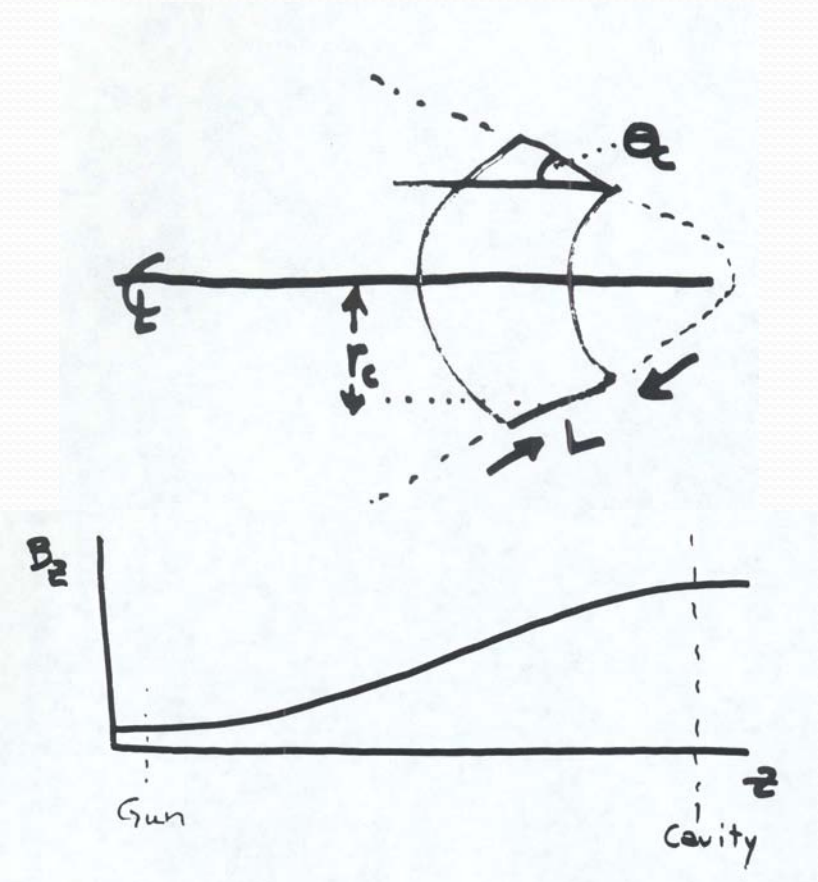

$$A = 2\pi r_c L$$

$$= 2\pi \frac{K r_c^2}{\sin\theta_c} \quad \left(K \le 1\right)$$

$$I = \left(\frac{I}{A}\right) A = J \frac{2\pi K r_c^2}{\sin\theta_c}$$

$$\square \frac{2\pi K J}{\sin\theta_c}\left(\frac{B_f}{B_i}\right) r_{gf}^2$$

$$Want\ J < 5 A/cm^2$$

Cathode Angle

Large Cathode Angle Gives:

- More Laminar Beam
- Less Beam Current
- Large Guiding Center Spread

Mod Anode Voltage Limits

- If V_1 is too high:
  Either the electrons strike the anode or arcing occurs (E>200 kV/cm)
- If V_1 is too low:
  $\alpha = v_\perp / v_{||}$ is too low for proper gyrotron operation

Temperature Limited Operation

- Currently, MIGs are operated temperature limited ($J_c/J_L << 1$)
  The above results from requiring E constant along the emitter
  Adds noise problem, also problems with high repetition rate.

The other area of concern in gun design involves the associated velocity spread which adversely affects gyrotron performance. Effects which result in beam spread include.

(1) beam space charge effects

(2) variation of initial cathode radius due to beam thickness

(3) nonadiabatic fields

(4) cathode surface roughness

(5) violation of axial symmetry in the electric and magnetic fields

(6) initial thermal spread due to finite cathode temperature

(7) nonuniform fields near the cathode

Electron Gun: Heated Emitter Ring/ Cathode

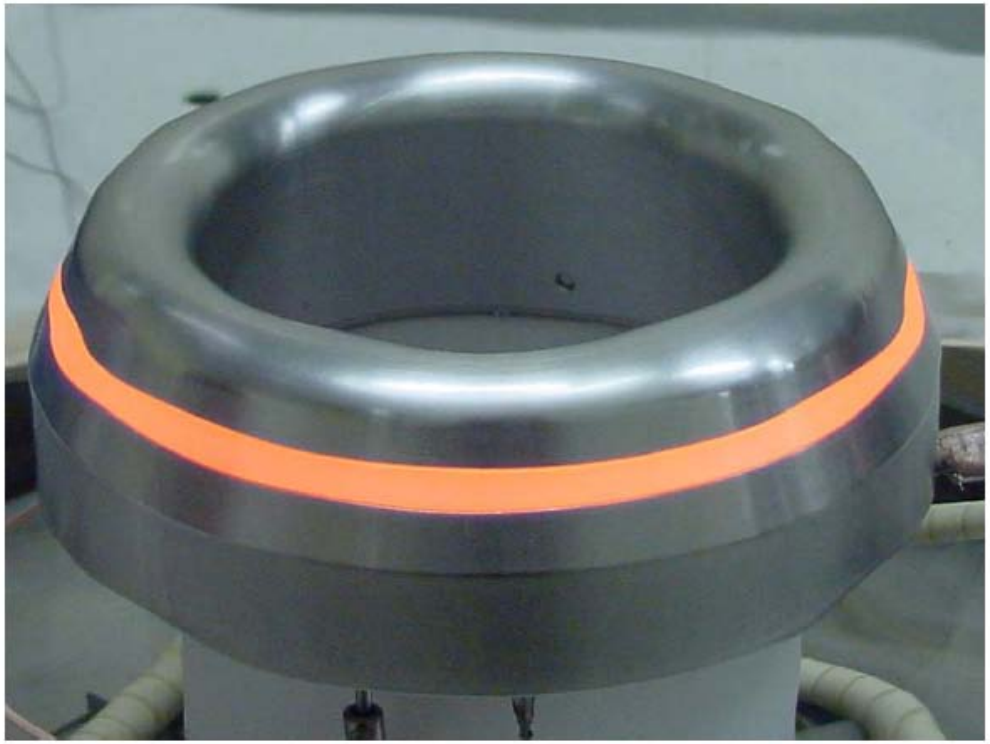

Note: The emitter ring, heated to about 1300°C, is operated here in an evacuated glass chamber.
The view through the glass makes it appear irregular, but in fact it is perfectly circular.

Example: 140 GHz 1 MW Gyrotron for W7-X

operating parameters

acceleration voltage U_{acc}	81 kV
beam current I_b	40 A
beam energy	3.25 MW
emitter current density j_e	2.5 A/cm^2
emitter radius R_e	50 mm

in the interaction region (cavity):

beam radius R_b	10.1 mm
pitch factor $\alpha = v_\perp / v_\parallel$	1.4
perpendicular e$^-$ velocity $v_\perp$	0.43 c
parallel e$^-$ velocity $v_\parallel$	0.3 c

cathode with emitter ring

$U_{cathode}$ and heater contacts

Beam tunnel

The beam tunnel suppresses unwanted parasitic oscillations

Magnetron injection gun (triode MIG) with beam tunnel

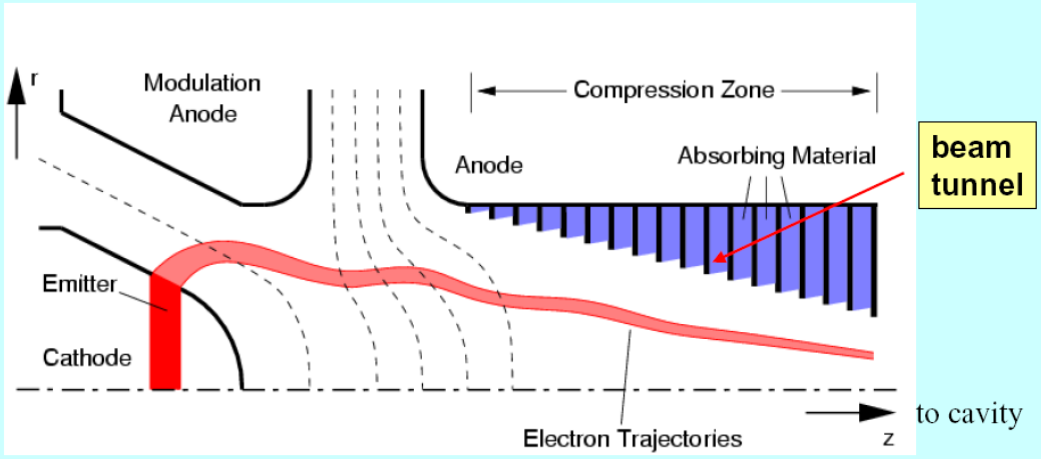

3D view of a beam tunnel

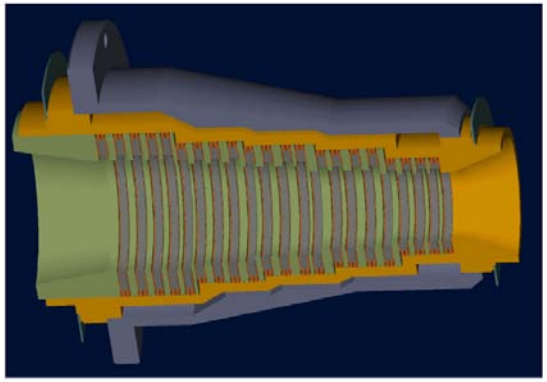

Beam tunnel with alternating copper discs and absorbing ceramic disks

EGUN Introduction

- EGUN, which is developed by Stanford Linear Accelerator Center, is designed to compute trajectories of charged particles in electrostatic and magnetostatic fields, including the effects of space charge and self-magnetic fields.
- Either rectangular or cylindrical symmetry may be used. It is a 2.5 dimension code meaning 2-D in all fields and 3-D in all particle motion. A Poisson's Equation Solver is used to find the electrostatic fields by using difference equations derived from the boundary conditions.
- Magnetic fields are to be specified externally by the user, by using one of several methods including data from another program or arbitrary configurations of coils.

Flowchart of MIG Egun Simulation Routine

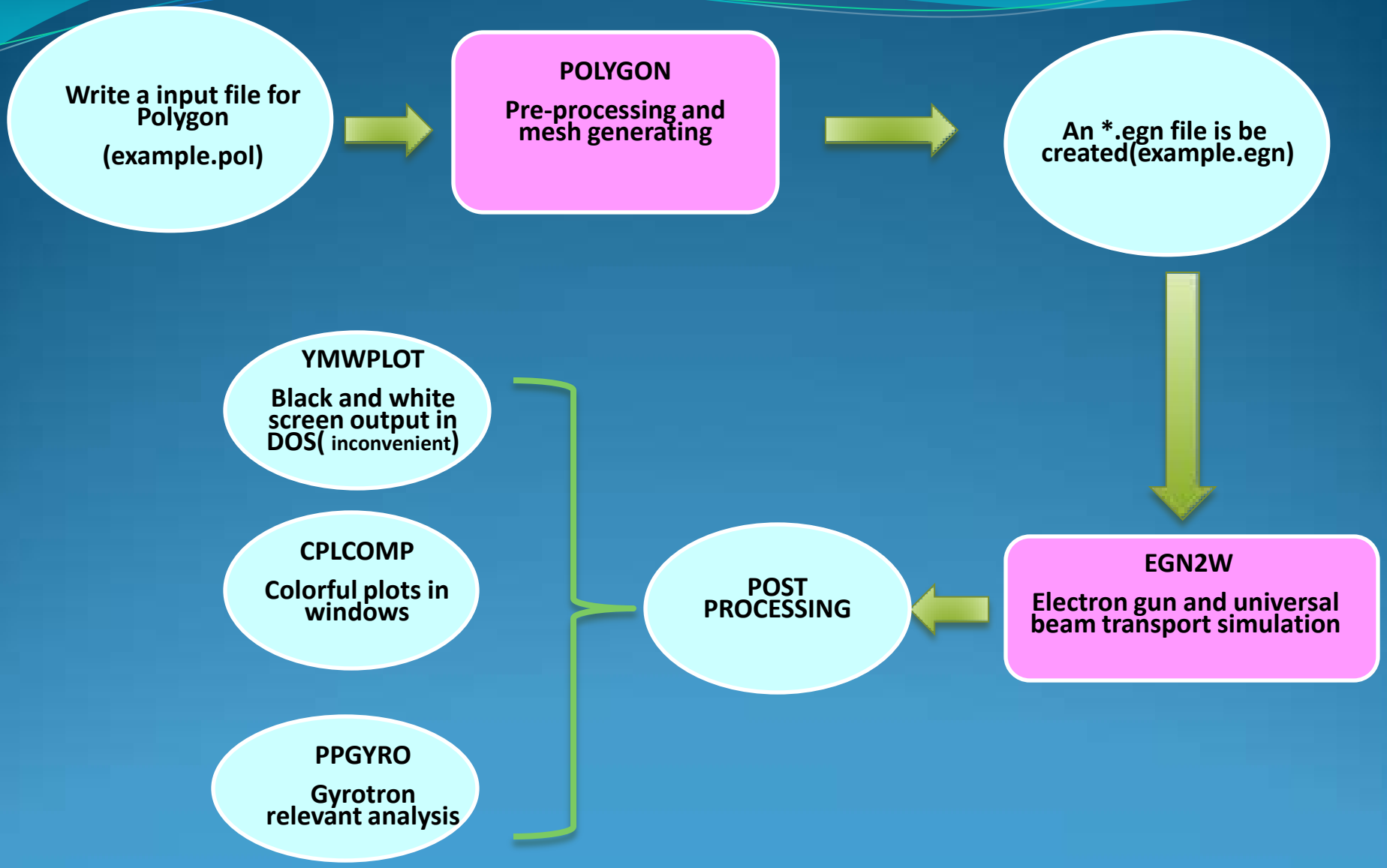

Magnetic Field Input

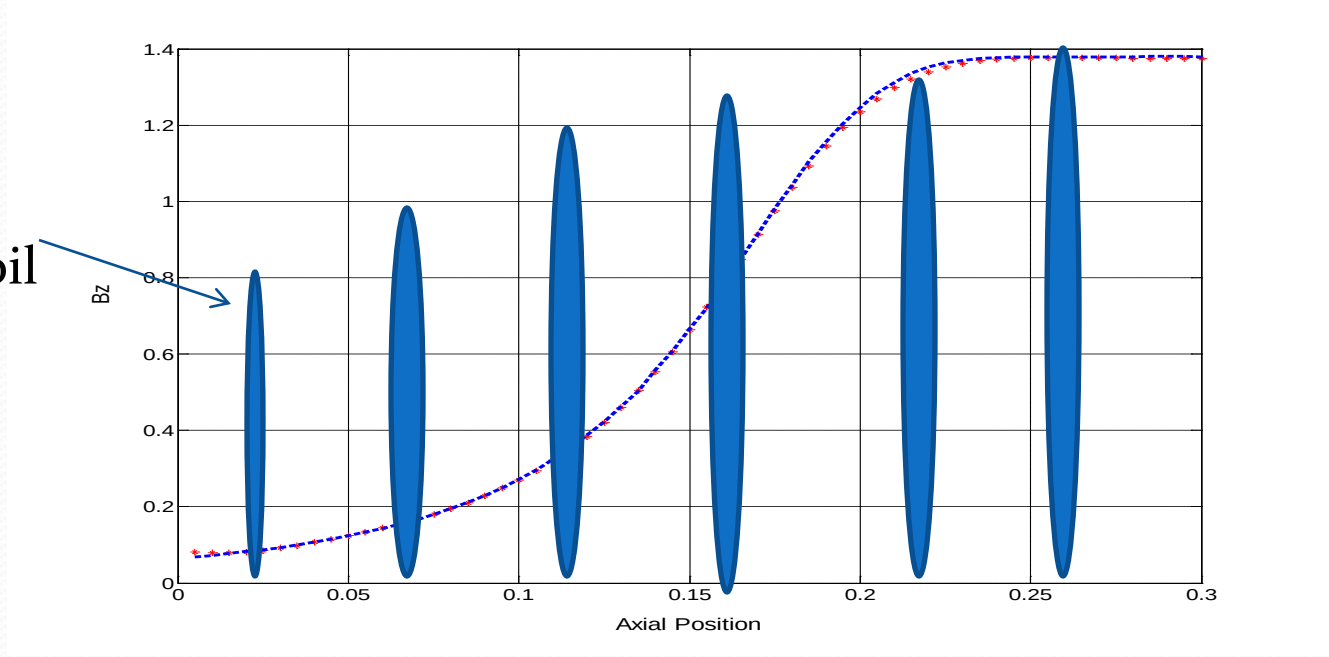

There are five methods of inputting magnetic field data in Egun. Two of them are very useful.

- By reading the full array fields on the axis, presumably as found by using another computer program such as Maxwell, CST-PS, Omnitrak and etc.. You can also write some simple codes to generate the data. I always use matlab to do this.
- By specifying ideal coils (radius, positions and strength)

Magnetic Injection Gun (MIG)

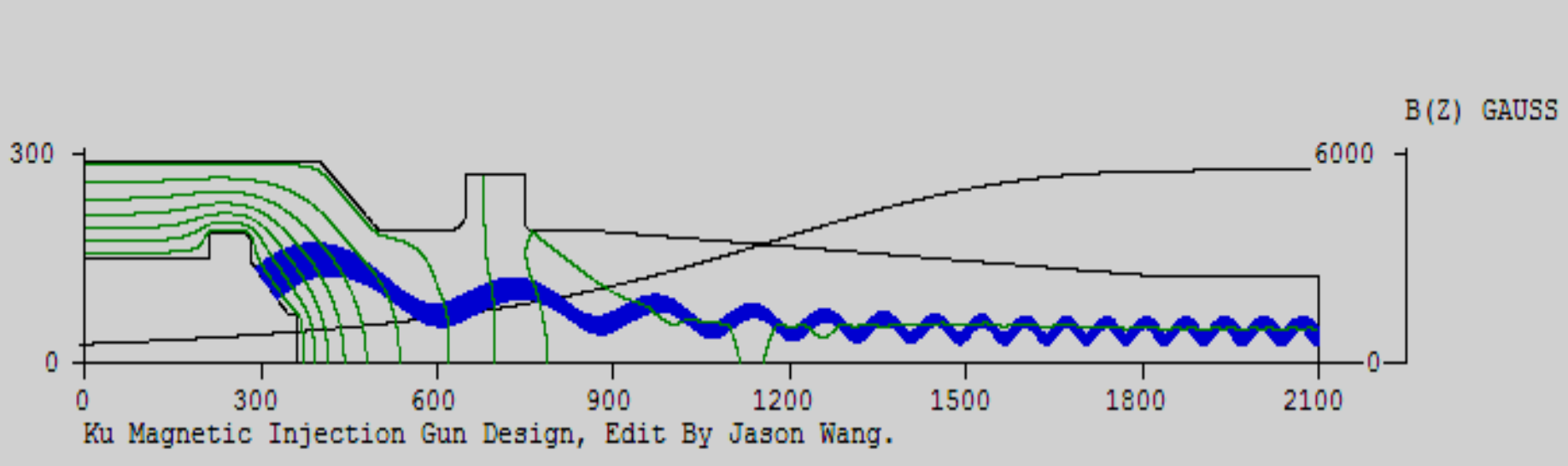

- After running egn2w, the results will saved in the *.out file. Then you can check the information of particles by PPGYRO. PPGYRO can give you the average and spread of perpendicular, parallel speed, guide center and beam alpha.
- Note: all positions and radii are given in mesh units, while velocities are in units of c.
- Use cplcomp to see the plots including electron distribution, beam density and etc..

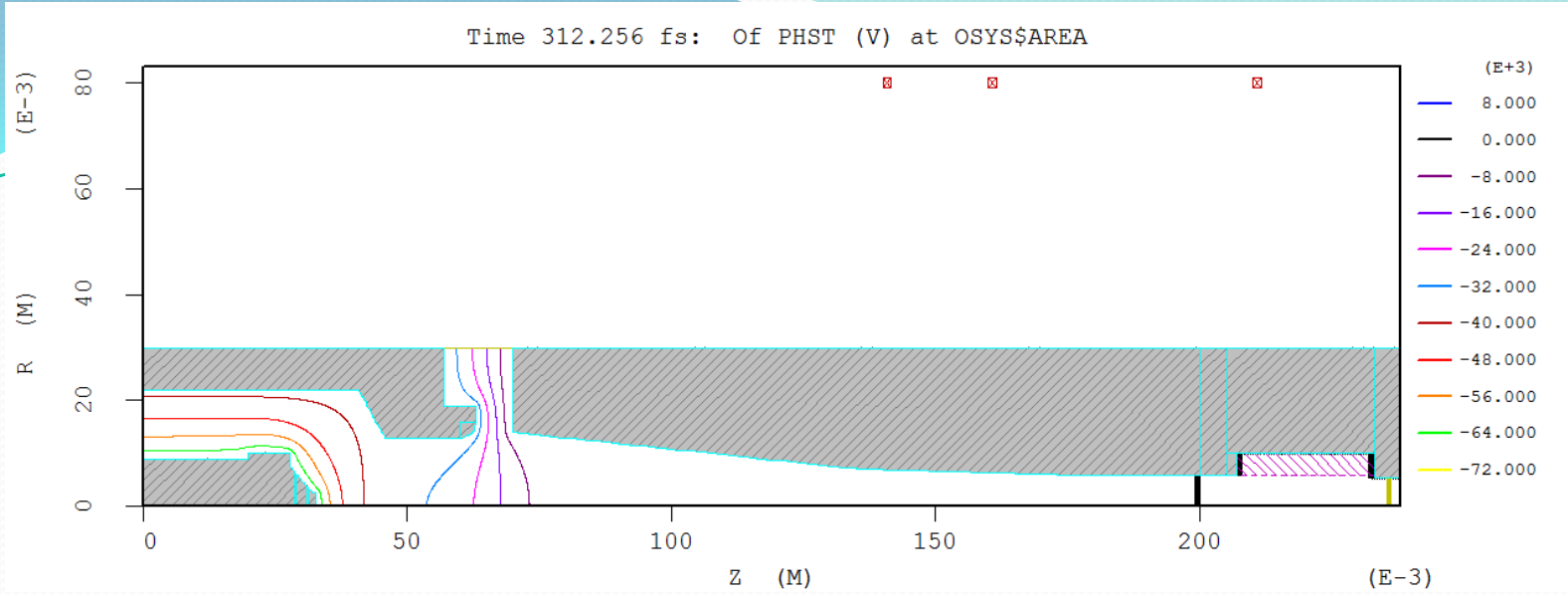

Electrostatic field distribution

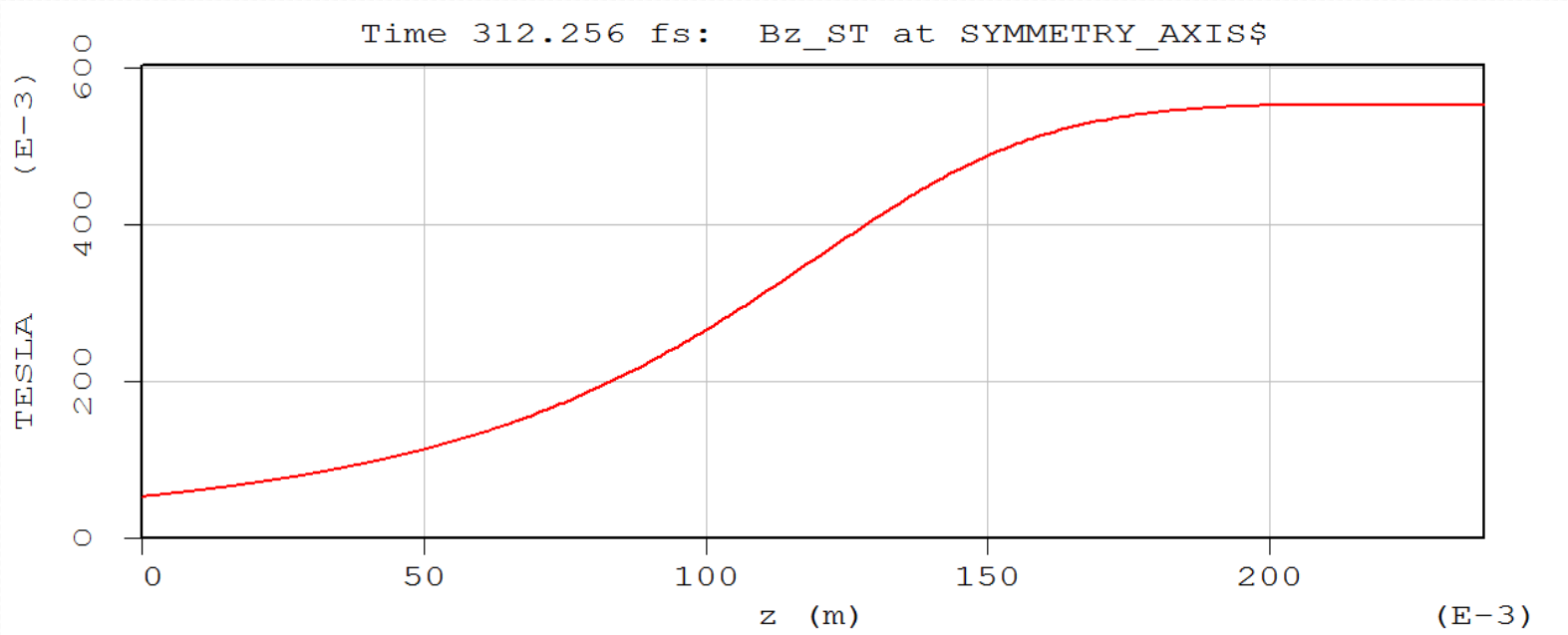

Bz distribution in axial direction

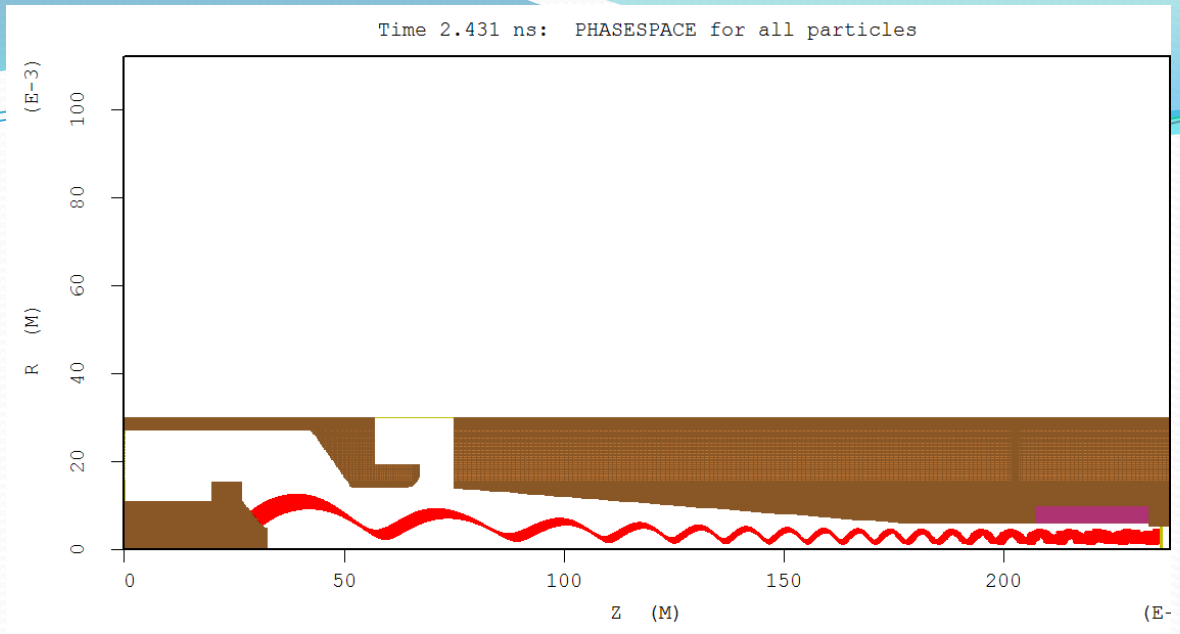

Beam distribution in axial direction

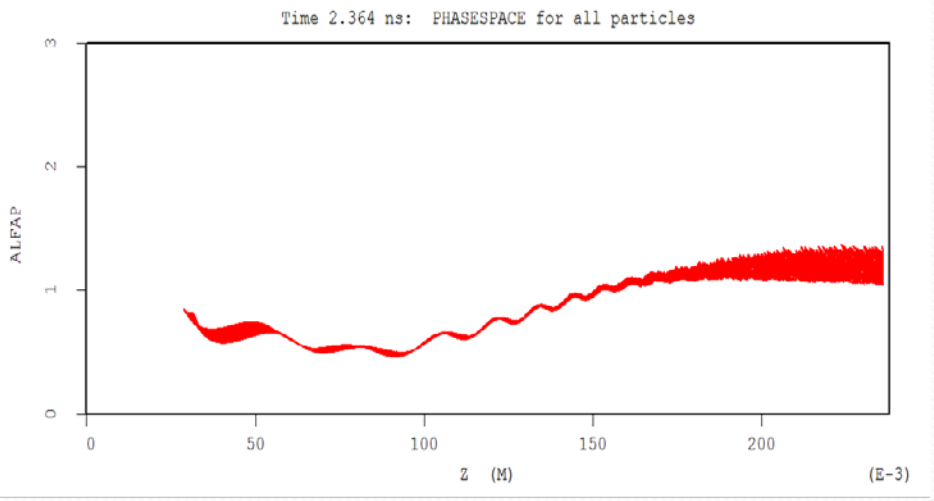

Beam velocity ratio(Vt/Vz) distribution in axial direction

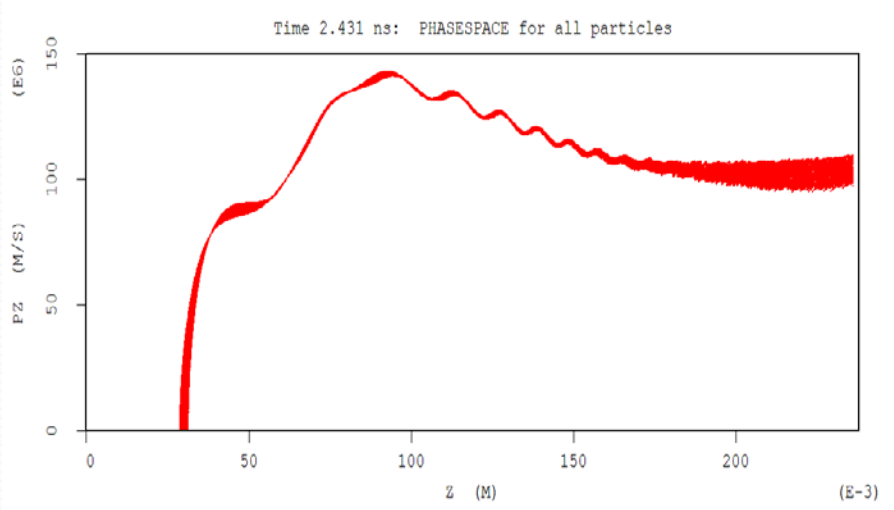

Pz distribution in axial direction

Depth of the potential wells (*Ariadne++*)

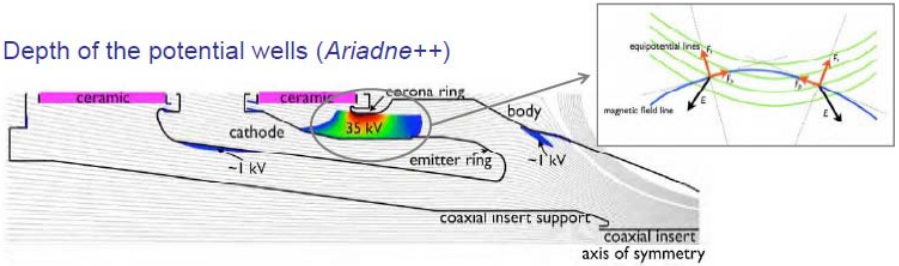

Trajectories of the electrons trapped in a magnetic mirror

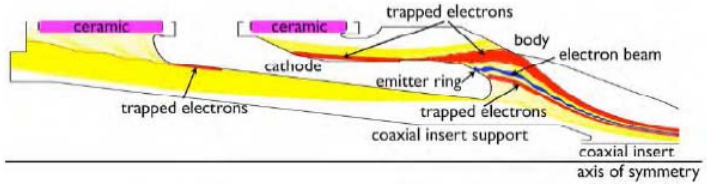

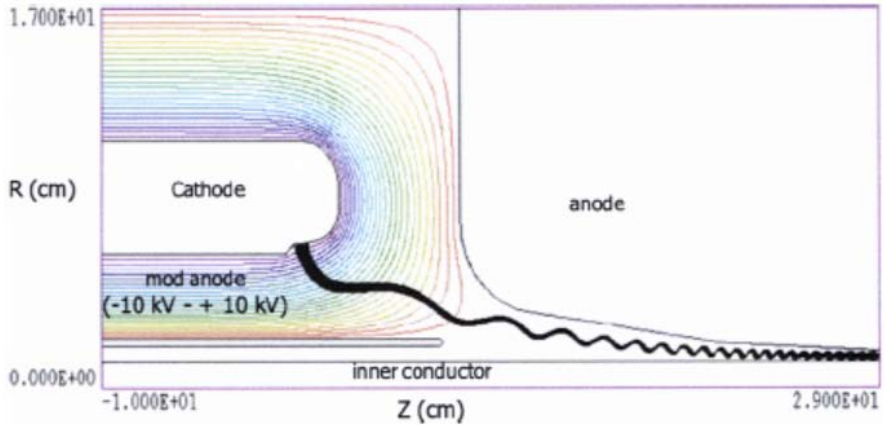

alpha of 1.4.

Figure 2. Conventional MIG designed for use with the 50 MW gyroklystron operating at the fundamental of the cyclotron frequency.

Production of an Axis Encircling Beam

The MIG concept is not the only technique which can be utilized to produce rotating electron beams for gyrotron interactions. As mentioned previously, large orbit axis-encircling beams can be produced by propagating hollow electron beams through magnetic steps. The major features of this design are the use of an asymmetric field reversal and initially converging electron beam which are said to reduce the length required for adiabatic compression of beam.

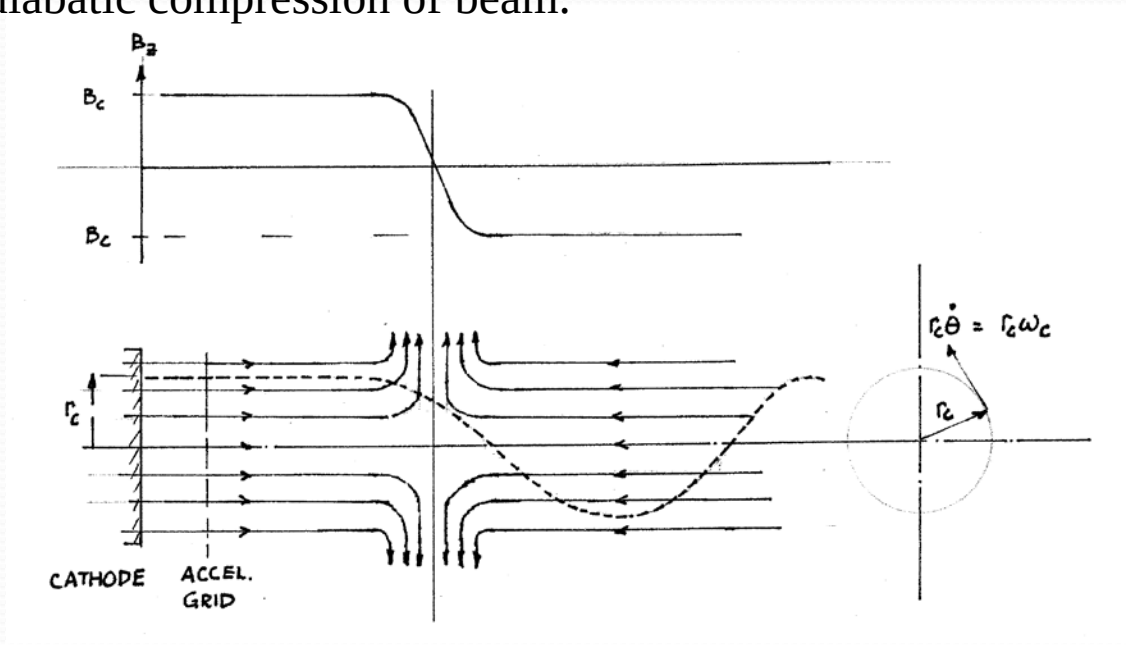

This is achieved by having at the cathode a uniform axial magnetic field which is of the same magnitude but of the opposite sense as the magnetic field downstream.

Theoretical Analysis

$$\dot{r}_{z_{out}} = \int_0^2 \frac{\omega_c}{2} \frac{f^2 - 1}{(4\eta^2 - q^2)^{1/2}} \frac{dq}{f'} \quad (1)$$

$$\dot{\theta}_{(z,r_0)} = \frac{\omega_c}{2} \left(f(z) - \left(\frac{r_0}{r} \right)^2 \right) \quad (2)$$

$$\dot{r}_{z_{out}} = \frac{\zeta \omega_c}{2} \sin^{-1} \frac{1}{\eta} + v_{r0}. \quad (3)$$

$$v_{r0} = -\frac{\zeta \omega_c}{2} \sin^{-1} \frac{1}{\eta}. \quad (4)$$

$$\frac{\dot{\theta}_{(z,r_0)} - \dot{\theta}_{(z,r_0+\Delta r)}}{\dot{\theta}_{(z,r_0)}} = \frac{2 r_0 \Delta r}{r^2 f(z) - r_0^2}. \quad (5)$$

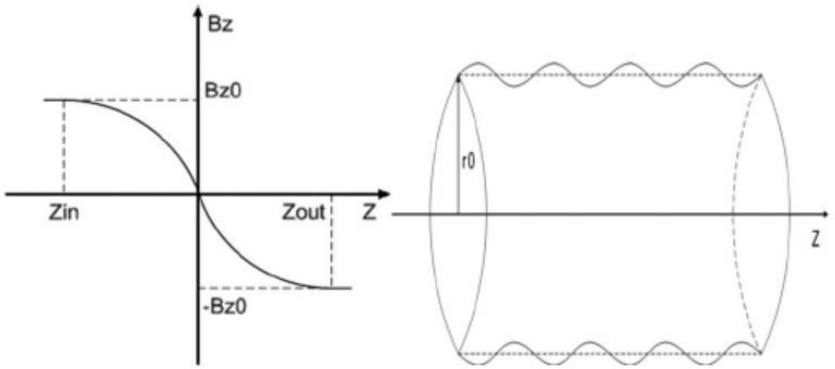

Nonideal cusp magnetic field and beam envelope with ripple.

The Lagrange equations are a convenient way to solve for the motion of the electron in various field configurations. We can get the Lagrange equations of the relativistic electrons motion when a beam passes through the cusp magnetic field. The velocity spread depends upon the thickness of the beam before it enters the cusp magnet. It is obviously impossible to use extremely thin cathodes due to the limitations of the emission density and the lifetime of the cathode.

Consequently, to achieve small beam velocity spread, one needs to compress the thickness of the beam after emission and before it passes through the cusp magnetic field.

Co-Simulation Approach and Tools

For the cusp gun design, the beam spread is not only dependent upon the dimensions of the anode, cathode, focus anode, and the voltage of each electrode, but also dependent upon the profile and the position with respect to the cathode. For a given magnetic field distribution, there may not exist, or at least be very difficult to find, the optimal dimensions for the desired beam quality. To increase the design efficiency and address the aforementioned problem, a new co-simulation method is developed.

First, the input file for Egun is generated by MATLAB, and the dimensions are parameterized.

Second, the magnetic field data results from Maxwell2D are taken automatically by the MATLAB code and then rewritten into a form which can be recognized by Egun.

Third, the new magnetic field data files are inserted into the Egun input file, and then Egun is called by the MATLAB code.

Fourth, the beam calculation results from Egun are analyzed by the MATLAB code. If the beam spread is not sufficiently small, then, the key dimensions will be swept to search for the minimum beam spread. As is well known, the distribution of the magnetic field is very critical for the design. Consequently, if the beam spread goal cannot be met, then the MATLAB code will call Maxwell2D to obtain a new magnetic field profile.

Finally, the aforementioned steps are repeated to obtain the optimized design. After the optimization is finished, the 3-D CST-PS code will perform a simulation of the magnet and cusp gun to check the results of the 2-D simulation and to study the effects of misalignment between gun and magnet.

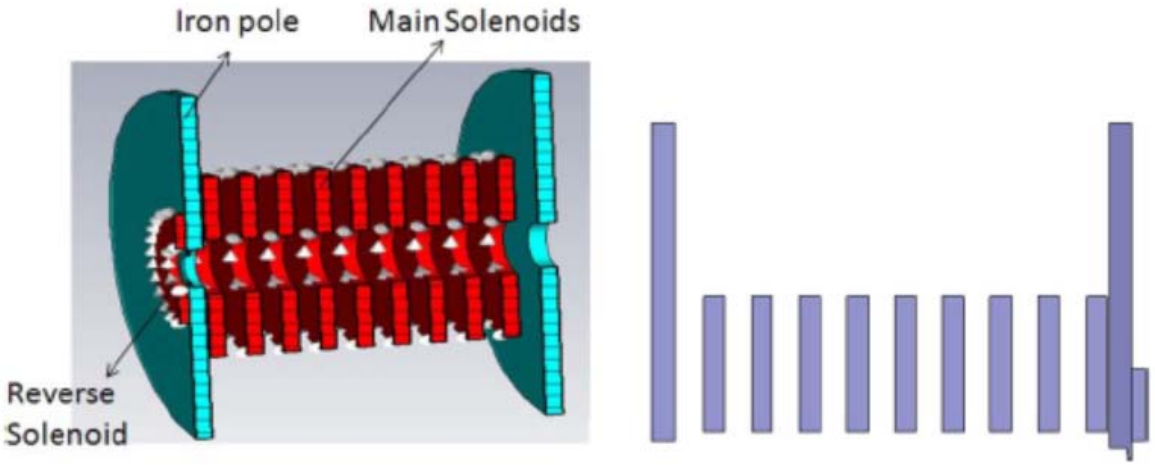

Structure of the magnet in CST-PS and Maxwell2D.

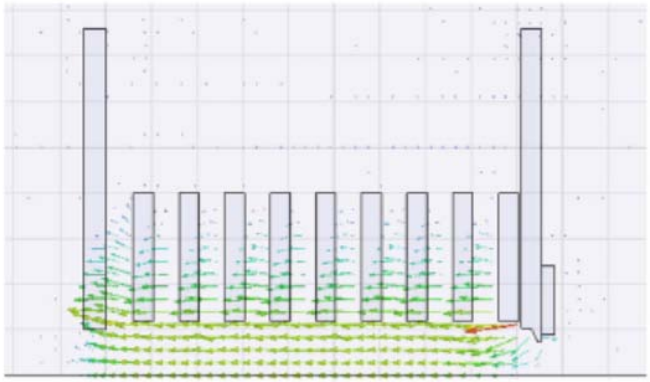

Magnetic field distribution of Maxwell2D and CST-PS simulation.

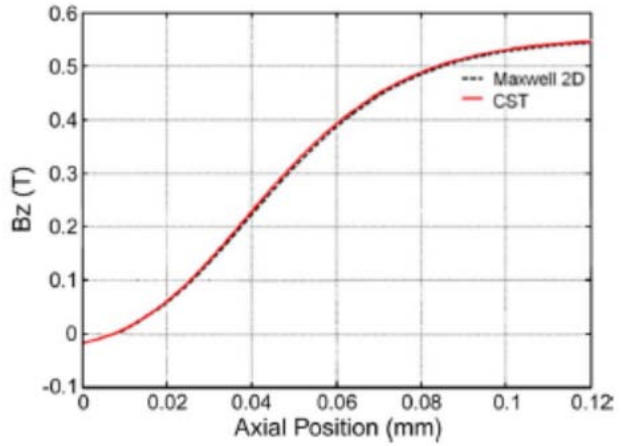

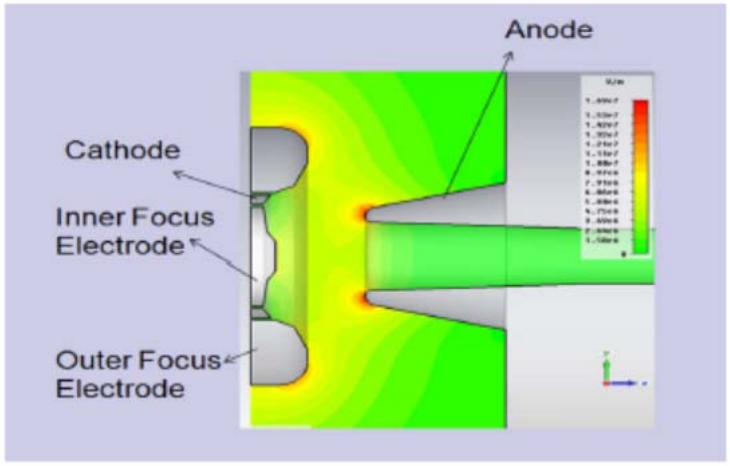

Fig. 4. Structure of the cusp gun and the electrostatic distribution.

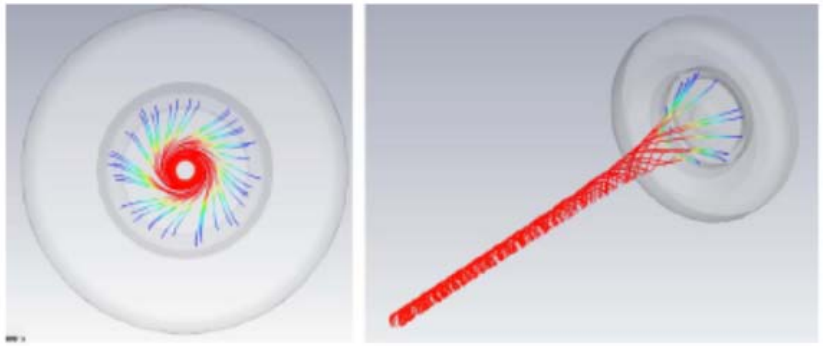

Fig. 6. Transverse and isometric views of electron trajectories.

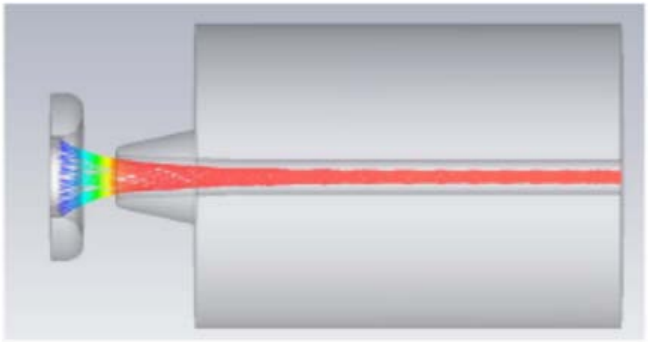

(a)

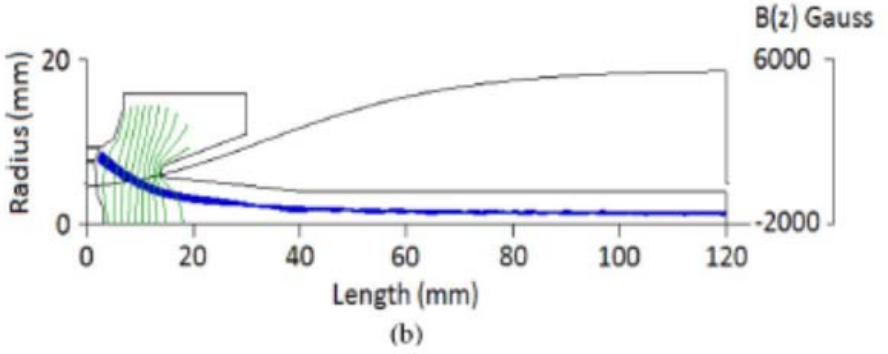

(b)

Fig. 5. Trajectory simulation results: (a) CST-PS 3-D result. (b) Egun 2-D simulation results including magnetic field distribution.

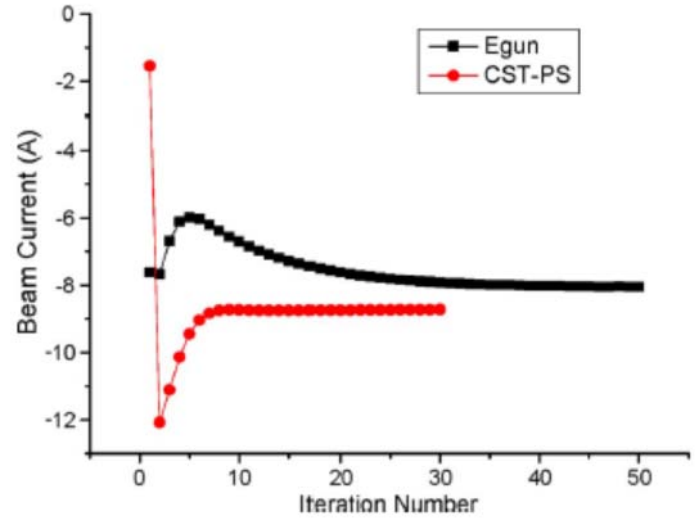

ig. 7. Beam current results of Egun and CST-PS.

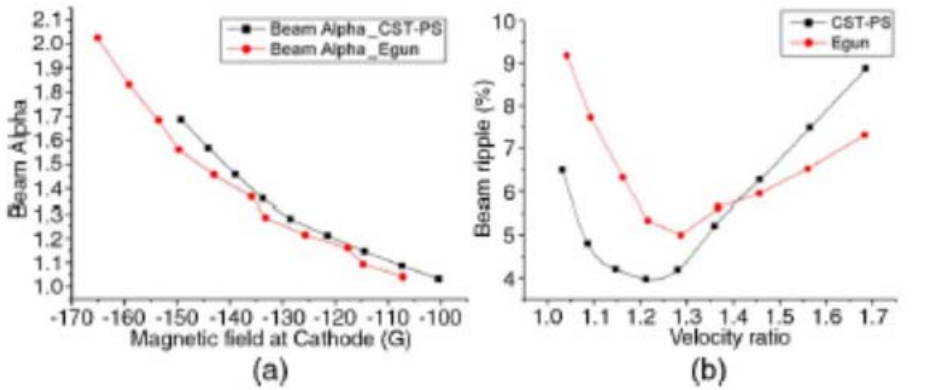

Fig. 8. (a) Beam velocity ratio versus the magnetic field at the cathode. (b) Beam ripple versus velocity ratio.

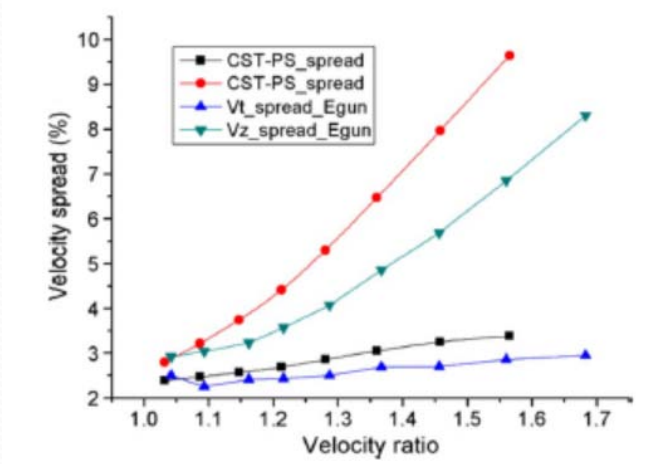

g. 9. Velocity spread versus the velocity ratio of Egun and CST-PS.

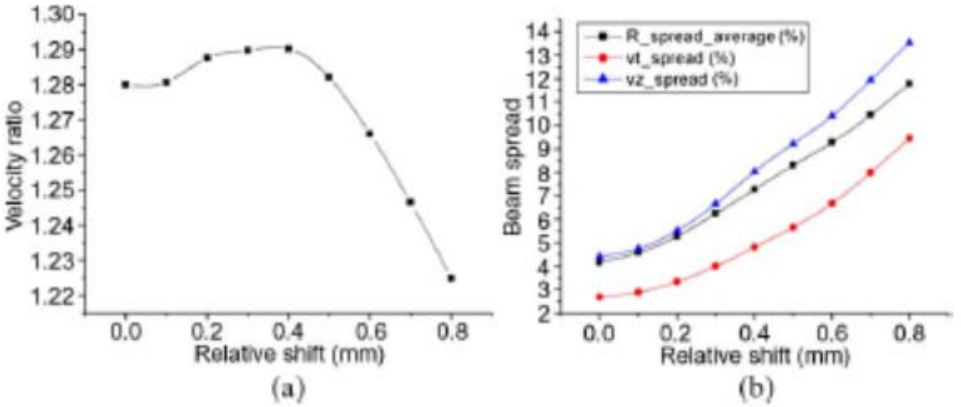

Fig. 11. Results of mismatch study. (a) Velocity ratio versus relative shift. (b) Beam ripple and beam velocity spread versus relative.

TABLE I
DESIGN AND SIMULATION RESULTS

Parameter	Value
Beam Voltage (kV)	70
Beam Current (A)	8
Cathode Radius (mm)	8.5
Maximum operating Magnetic field (T)	0.555
Cathode Loading (A/cm^2)	8.4
Velocity Ratio	1.0~1.8
Beam Ripple	5%~6%
Axial Velocity Spread	3%~6.5%
Perpendicular Velocity Spread	2.08%~2.82%

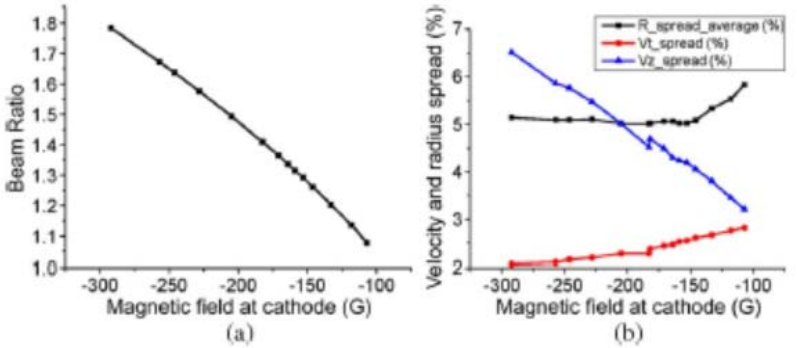

Fig. 10. (a) Velocity ratio versus magnetic field at cathode according to different reverse solenoid current. (b) The beam ripple and velocity versus the magnetic field at the cathode according to different reverse solenoid current.

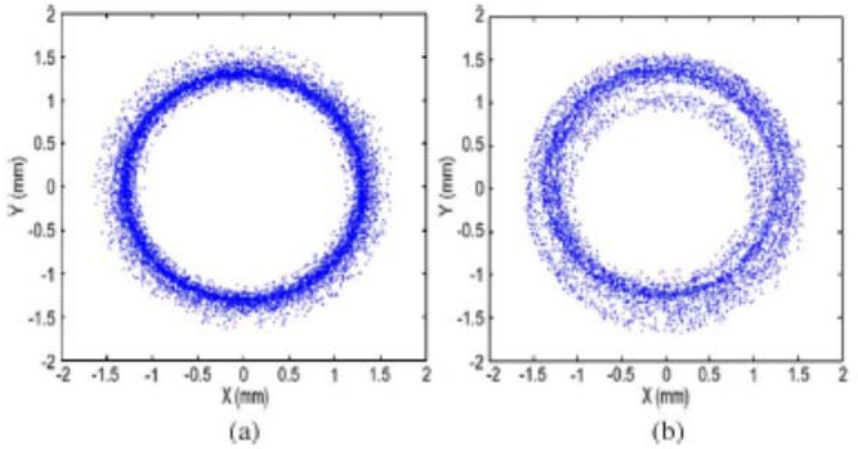

Fig. 12. Beam distribution on the cross section. (a) Without mismatch. (b) With a 0.8-mm relative shift.

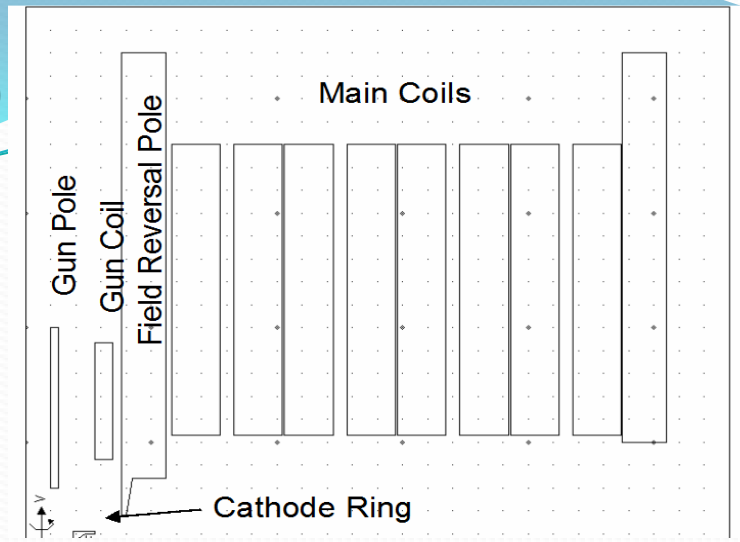

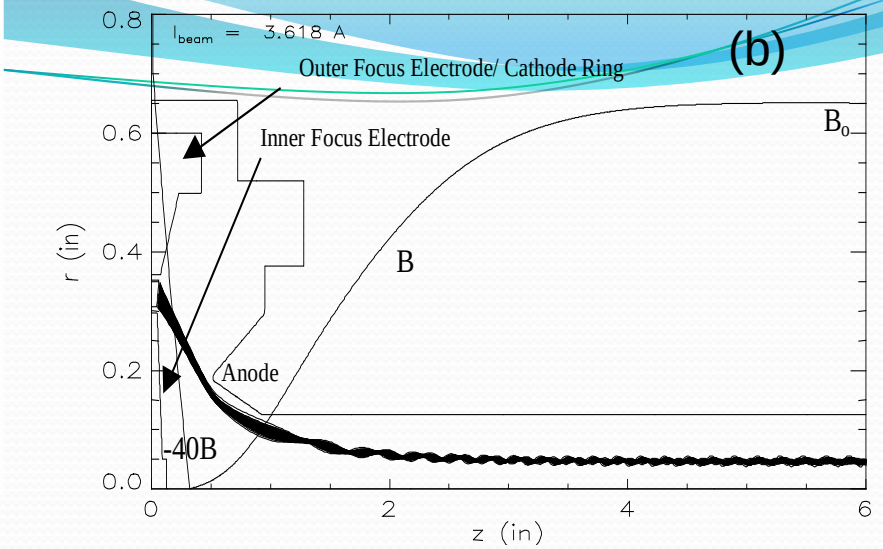

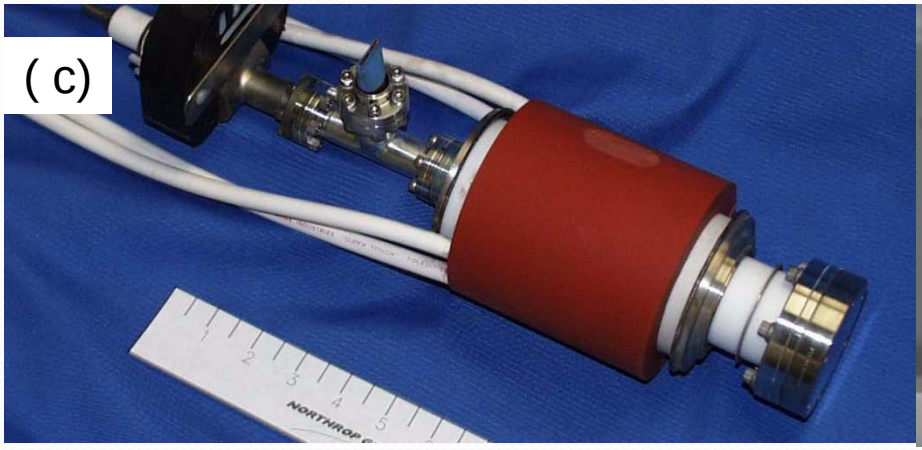

Cusp Gun developed by Northrop Grumman

- Axial Electron Beam Starts Spinning Due to v_z x B_r Force in Magnetic Reversal Region

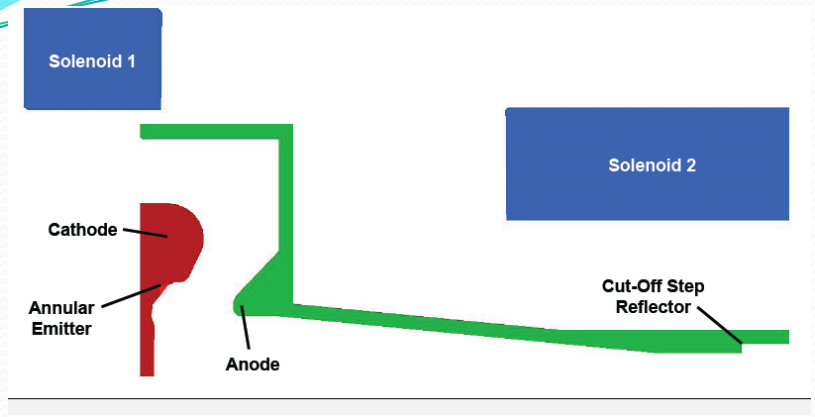

Cusp Gun Geometry

The magnetic field is crucial to cusp gun operation, particularly the tuning of beam alpha. In practice, the combination of electrostatic and magnetic focussing requires a smoother cusp transition in order to ensure good alignment of electron guiding centres.

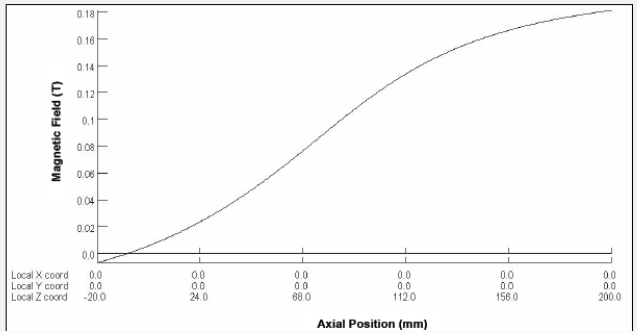

Magnetic field profile

Simulations of the electric field profiles at the electrodes were used to refine electron gun geometry so as to:

1) avoid emission from the focus electrodes.

2) minimise the risk of arcing.

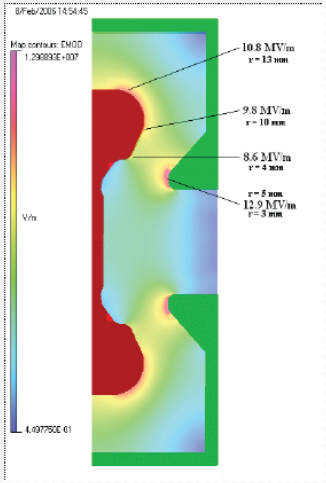

Electric Field Profile

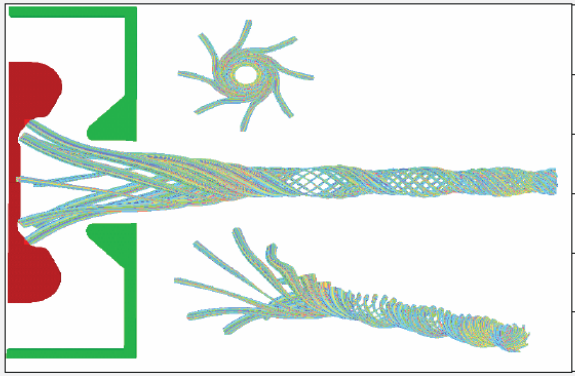

Beam Transport	100%
Beam Voltage	150kV
Beam Current	70A
Beam Power	~10MW
Alpha	1.2
Alpha Spread	<5%

Trajectories were simulated using the finite difference code OPERA-3D, the PIC code MAGIC and the finite difference code SureTraj.

Simulated Electron Trajectories

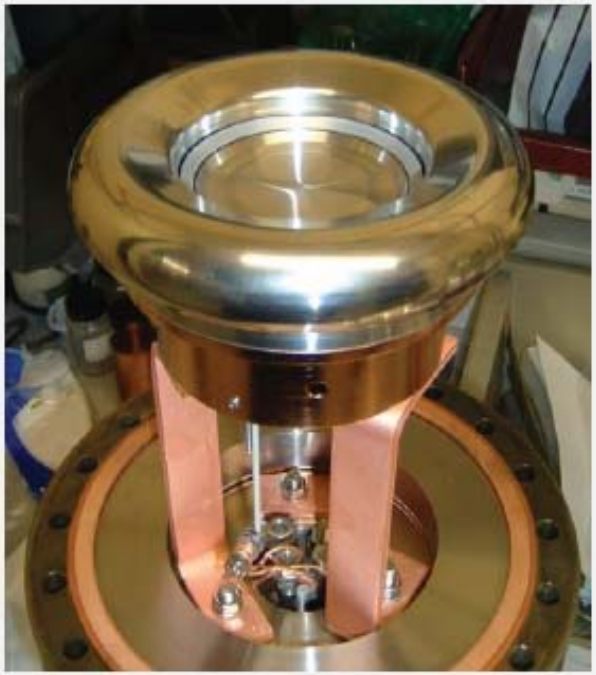

Thermionic cathode and focus electrodes.

Completed thermionic cusp electron gun.

Gyrotron Cavities

Resonator (Cavity)

- Open waveguide resonator (hollow waveguide or coaxial)
- Downtaper at the electron entrance to minimize rf power traveling towards the gun: The operating mode is reflected.
- Non-linear uptaper at the exit to increase the diameter

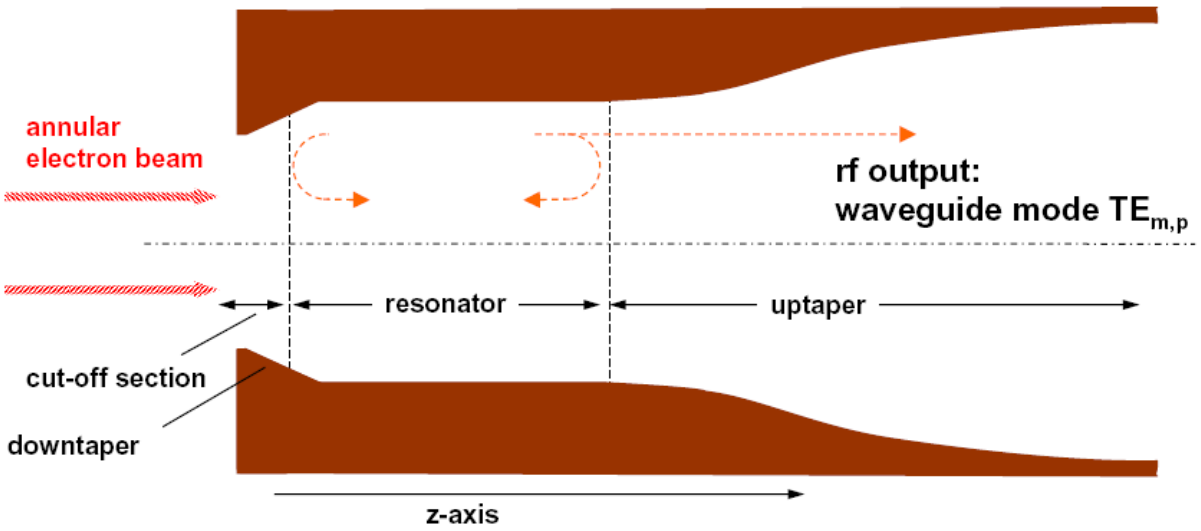

The electron beam enters the cavity from the left, because of the downward taper, the resonating mode is cut-off at position z_1.The cavity fields, therefore, build up until balance is achieved between the power extracted from the electrons and that dissipated in the walls and that coupled out of the open end.

The approach to solving for the cavity parameters is to locally (in z) expand the fields in a complete set of orthogonal transverse electric modes for each of two polarizations. In general, the modes are coupled through the changes in the waveguide cross section with axial position as modified by the presence of the electron beam. This results in an infinite set of one-dimensional coupled equations resembling the familiar transmission line equations.

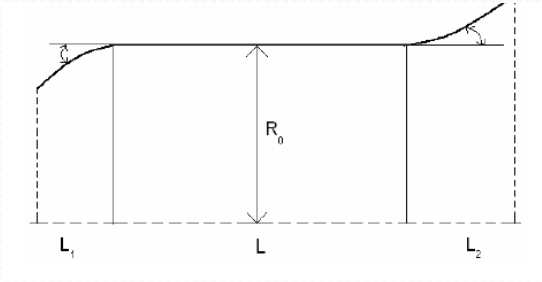

Gyrotron cavity resonator

For cylindrically symmetric resonators with only varying cross sections, the equations simplify considerably in the absence of the electron beam. In particular, the TE_{mn} modes are essentially uncoupled greatly facilitating the solution. It can be shown that in this case the axial dependence of the electric field intensity is given by

$$\frac{d^2E(z)}{dz^2}+\left[\frac{\omega^2-\omega_{co,eff}^2(z)}{c^2}\right]E(z)=0$$

In the above, the effective cutoff frequency, local cutoff frequency and wall function are given respectively by $\omega_{co,eff}^2(z)=\omega_{co}^2(z)\left[1-m^2W_L(z)/q_{mn}^2\right]$ $\omega_{co}^2(z)=c^2\,q_{mn}^2/a^2(z)$

and

$$W_L(z) = \left\{ \left[a'(z) \right]^2 \frac{\left(q_{mn}^2 - 2m^2 \right)}{\left(q_{mn}^2 - m^2 \right)^2} - \frac{a''(z)a(z)}{\left(q_{mn}^2 - m^2 \right)} \right\}$$

where the prime indicates the spatial derivative. The eigen functions appropriate to the cavity resonances must satisfy together with the following boundary conditions

$$\frac{dE(z)}{dz} - k_{in}E(z) = 0 \text{ at the electron gun end } (z = z_{in}) \text{ and}$$

$$\frac{dE(z)}{dz} - ik_{out}E(z) = 0 \text{at the output end } (z = z_{out}).$$

In the above, $k_{in} = \left[\omega_{co}^2 (z_{in}) - \omega^2 \right]^{1/2} / c$

and $k_{out} = \left[\omega^2 - \omega_{co}^2 (z_{out}) \right]^{1/2} / c$

The above choice ensures cutoff fields at the input and propagating fields at the cavity output. Often a simpler input boundary condition [$E(z_{in}) = o$] is employed due to the rapid fall-off of the fields within the cutoff section. In addition, the initial phase of the cavity fields $\phi(z)$ is normally set equal to zero at the cavity input end and remains relatively small due to the partial standing wave nature of the cavity fields. In the output section, the phase varies appropriately for a traveling wave.

From the cavity stored energy ε_m and output Poynting flux S_{out} may be obtained. The former is given by

$$\varepsilon_m = \frac{J_m^2\left(k_{mn}\right)\left(1-m^2/k_{mn}^2\right)a_o^2}{8}\int_{z_{in}}^{z_{out}}\left|E\left(z\right)\right|^2 dz$$

where a_o is the maximum cavity radius and $S_{out} = 2\omega_I\varepsilon_m$ with ω_I the imaginary part of the cavity eigenvalue. It is also helpful to define the diffraction Q through the relation

$$Q_D = \frac{\omega_R\varepsilon_m}{S_{out}} = \frac{\omega_R}{2\omega_I}$$

where ω_R is the real part of the eigenvalue.

Then we can get $$Q_D = \omega_R t_c \approx \frac{4\pi\left(L/\lambda_R\right)^2}{1-\left|R\right|}$$

where λ_R is the free space wavelength corresponding to ω_R.

Taking |R| = 0 results in the lowest possible diffraction Q. Assuming a sinusoidal axial mode distribution permits S_{DIFF} to be written as

$$S_{DIFF} = \frac{p_c\left(1-\left|R\right|\right)J_m^2\left(q_{mn}\right)\left(q_{mn}^2-m^2\right)}{\left(L/\lambda_R\right)64\pi^2}\left[\frac{\lambda_R^2}{2}\right]$$

Using conventional techniques, numerical solutions may be found to the above relations computed. Figure shows results for the field profiles obtained for two different cavity arrangements (straight and tapered). Here, $E_R(z)$ and $E_I(z)$ correspond to the real and imaginary components of the complex electric field. Note the expected transition from partially standing to traveling wave and the more Gaussian-like profile for the tapered cavity.

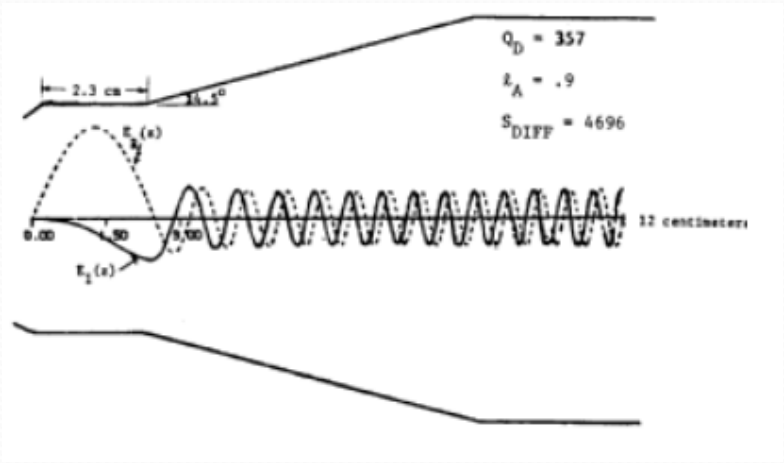

Field solution in straight cavity.

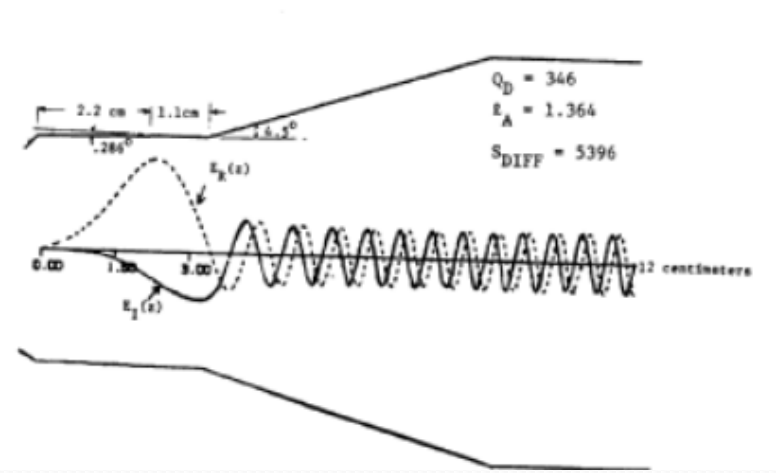

Field solution in tapered cavity.

Gyrotron Cavity Example

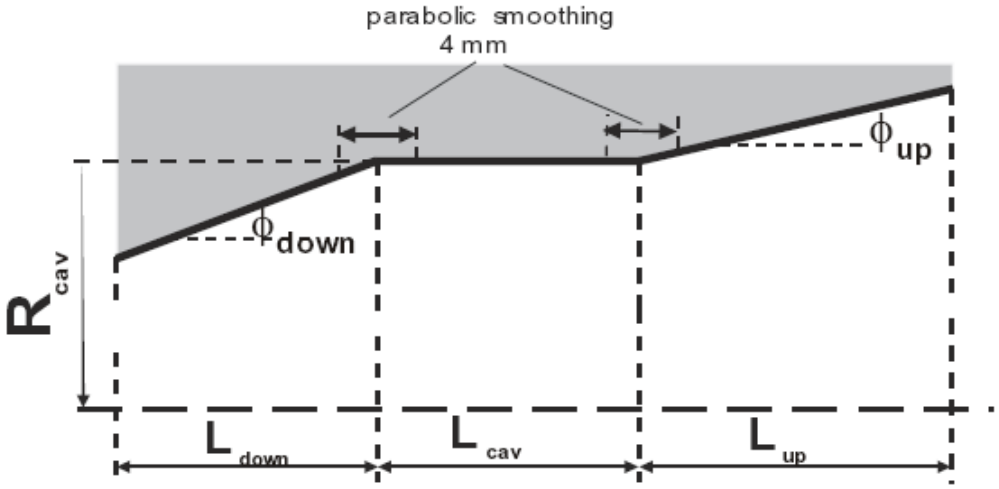

example for 1 MW, 140 GHz (λ_0= 2.14 mm) gyrotron:

- L_{cav} = 14.5 mm
- R_{cav} = 20.48 mm
- R_{beam} = 10.1 mm
- quality factor = 855 (cold)

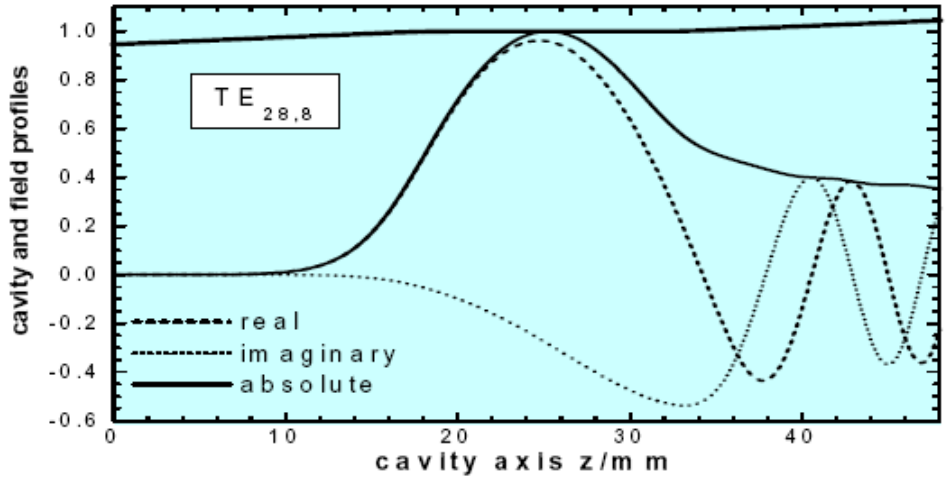

Field distribution in the cavity region

Cavity Mode Spectrum

MW gyrotrons use higly overmoded resonators -> dense spectrum of relevant modes

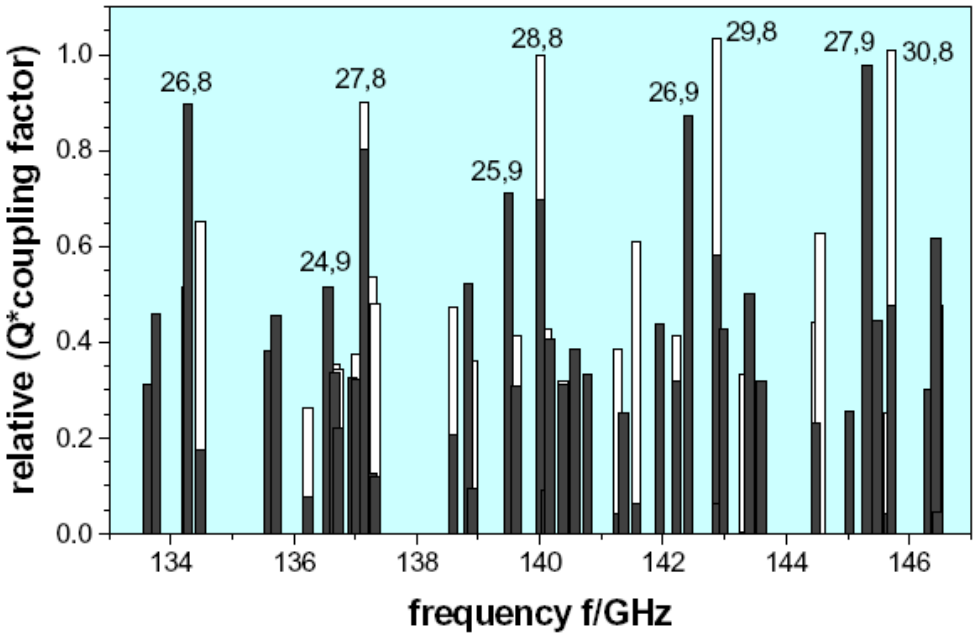

wall losses @ 1 MW: ~ 2 kW/cm^2

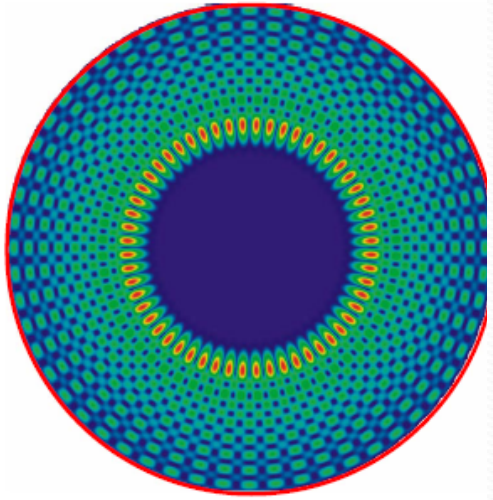

$TE_{28,8}$ mode

The other loss mechanism is ohmic dissipation in the cavity walls. This can be expected to be lower than that of a closed cavity because of the absence of the end walls. The other competing factor is the increased wall resistivity due to factors such as mechanical stresses and surface roughness. The total cavity Q is then given by

$$Q_{total}^{-1} = Q_d^{-1} + Q_\Omega^{-1}$$

It is common to define a circuit efficiency η_c given by

$$\eta_c = 1 - Q_{total}/Q_\Omega = Q_\Omega/\left(Q_\Omega + Q_d\right)$$

For high power cw gyrotrons, one wishes high efficiency implying operation with $Q_d << Q_\Omega$. Conversely, for low power devices it may be desirable to minimize the start oscillation thereby dictating parameters appropriate to $Q_d >> Q_\Omega$.

For particularly complicated structures or cavities where the dimensions change rapidly, the preceding formalism is inadequate. In the case of structures which still possess cylindrical symmetry, another approach is available. Here, one can employ a computer program such as SUPERFISH, HFSS and CST which solves for the electromagnetic eigen modes.

At extremely short wavelengths under high average power operations, the cavity wall loads becomes a significant limiting factor. In order to extend high power gyrotron operation to shorter wavelengths, a number of groups have been pursuing quasi-optical approaches. A schematic of a quasi-optical cyclotron maser is shown. By employing mirrors of sufficiently large dimensions, the resonator power loading can be reduced to levels which can be dissipated using conventional cooling techniques which still utilize high electron beam power.

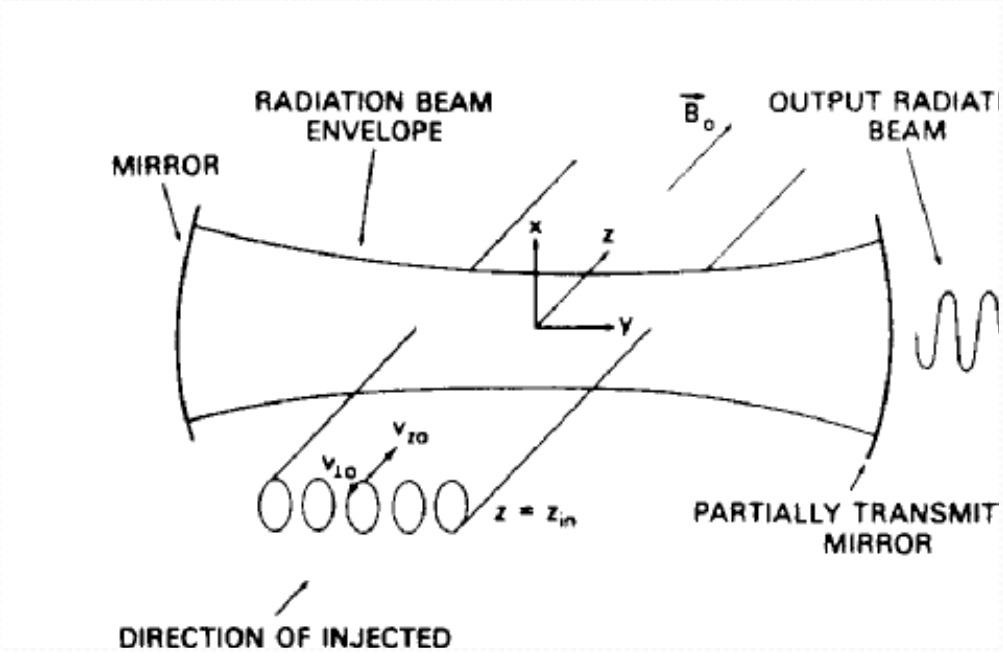

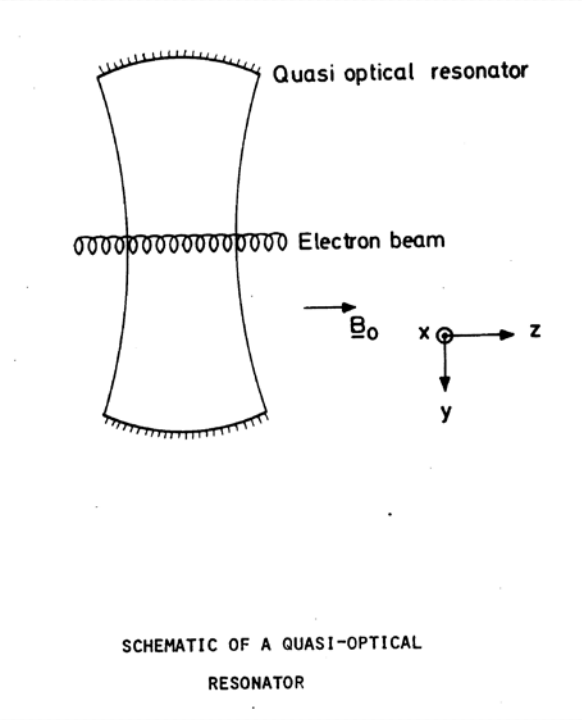

Schematic representation of the quasioptical electron cyclotron maser. The electron beam propagates along and rotates about the z axis and the radiation beam axis coincides with the y axis.

The possibility of fine wideband frequency tuning

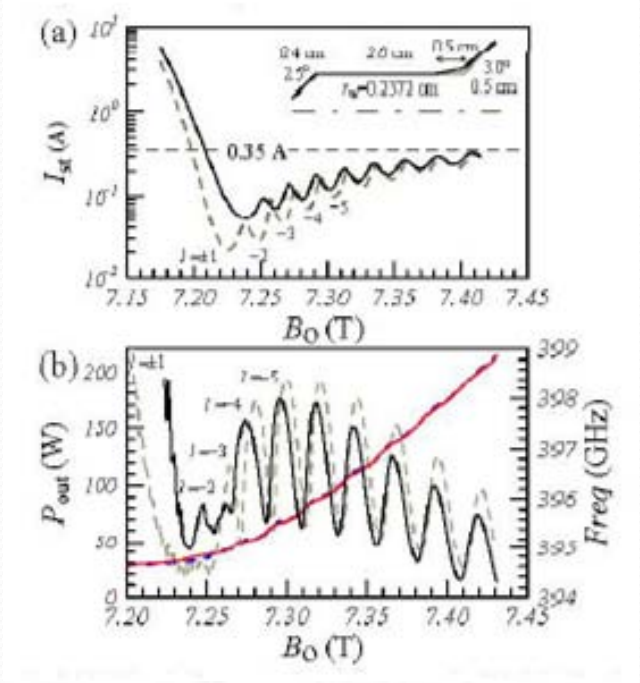

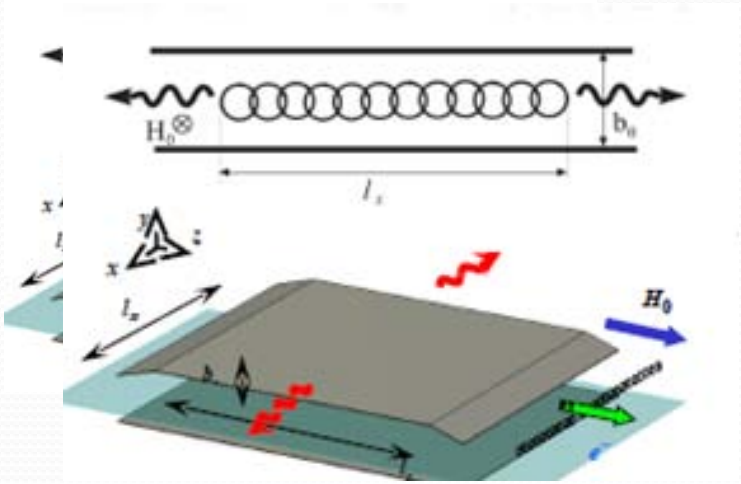

280 GHz gyrotron
with quasi-optical cavity

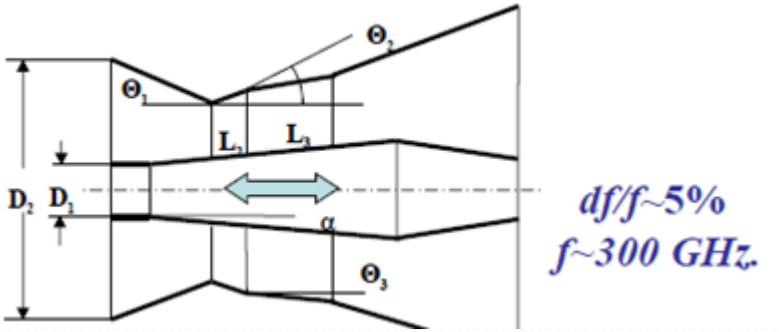

df/f~5%
f~300 GHz.

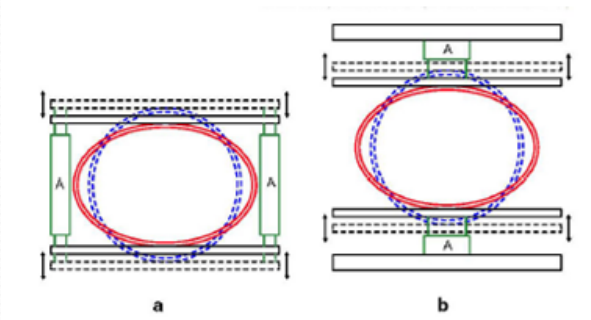

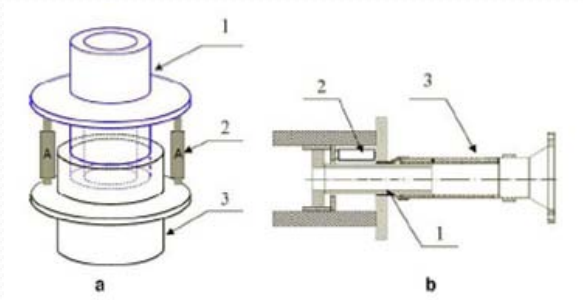

Gyroklystron

Frequency(GHz)	Beam Voltage(kV)	Beam Current(A)	Output Power(MW)	Efficiency	Gian(dB)
8.6	500	470	85	32%	30
9.87	425	150	24	33%	34
17.1	460	540	100	37.4%	60
17.14	500	720	158	41%	
19.1	437	232	29	27%	15
22.8	500	367	68	37%	
30	500	300	68	45%	45
30			6.5	25%	30
91	500	55	10.5	38%	58

Compact Linear Collider (CLIC) with a reasonable length, a high accelerating gradient and high RF frequency are required. **A** gyroklystron in the frequency range of 30 GHz is considered to be one of the most promising RF sources. The technical risk factors and achievable performance for several distinct configurations, including coaxial and cylindrical cavities interacting at the fundamental and second harmonic of the cyclotron frequency, and high power MIG gun all should be investigated in the study.

Why Gyroklystron?

Magnetron

Klystron

Gyroklystron

TM010 Mode: qmn=2.4

$$r_c = \frac{\omega q_{mn}}{c}$$

$$P_{\max} \propto r_c^2$$

TE01 Mode: qmn=3.83
TE02 Mode: qmn=7.01
TE53 Mode: qmn=13.99
TE73 Mode: qmn=16.53

$P_{\max\_klystron}$

$2.55 * P_{\max\_klystron}$

$8.53 * P_{\max\_klystron}$

$33.98 * P_{\max\_klystron}$

$47.44 * P_{\max\_klystron}$

Design of a Ka Band 450KW Gyroklystron

$$\frac{dp}{d\xi} + ip\left(\Delta + |p|^2 - 1\right) = -if_s F_s \exp(i\varphi_s)$$

$$\frac{dp}{d\xi} + ip\left(\Delta + |p|^2 - 1\right) = 0$$

$$p(\xi = 0) = p_{in1} = \exp(in\varphi_0), 0 \le \varphi_0 \le 2\pi$$

$$\delta_1 - i + I_1\chi_1 = \frac{2}{F_1}(I_1 P_{in}/P_{0\perp})^{1/2} \exp\left[i(\varphi_{in} - \varphi_1)\right]$$

$$\delta_s - i + I_s\chi_s = 0 \quad (s > 1)$$

$$\varphi_{in,4} = \varphi_0 - X_{14}\sin(\varphi_0) - X_{24}\sin(\varphi_{in,2}) - X_{34}\sin(\varphi_{in,3}) - \varphi_4 - \theta_{14}$$

$$\eta_{bun} = \left|\frac{1}{2\pi}\int_0^{2\pi} \exp(i\varphi_{in,4})d\varphi_0\right|^2$$

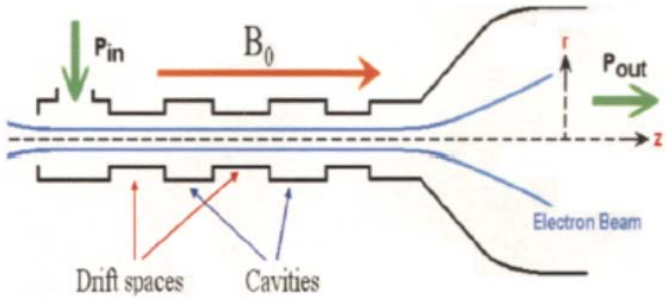

Fig.1 The layout of the gyroklystron cavity circuit consisting of four cavities separated by three drift spaces and an uptaper section.

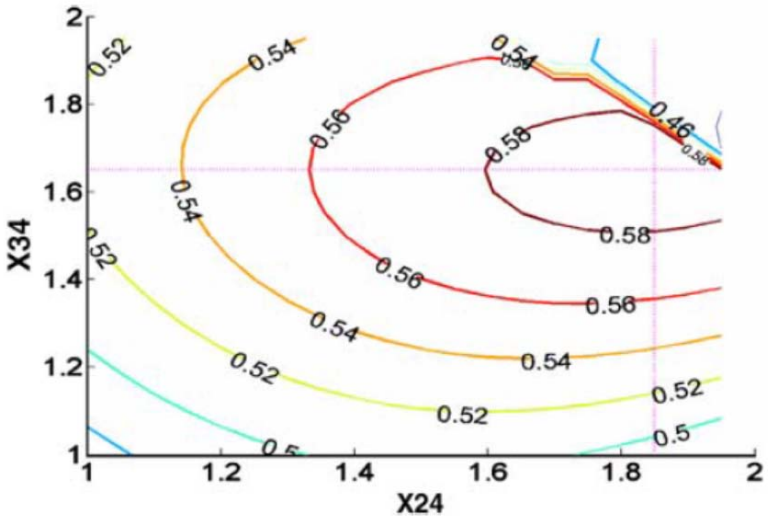

Contour plots of bunching efficiency

$$\nabla \times E + j\omega\mu H = 0$$

$$\nabla \times H - j\omega\varepsilon E = J$$

Maxwell Equation with current source

$$E = \mathrm{Re}\left\{aE_c e^{-i\omega t}\right\}$$

$$H = \mathrm{Re}\left\{a\frac{\omega_c}{\omega}H_c e^{-i\omega t}\right\}$$

Hot Cavity Fields

The expression for the time-independent amplitude

$$a = \frac{j\int J_\omega E^* dV}{\left(\omega - \frac{\omega_c^2}{\omega}\right)W_{EM}} \qquad W_{EM} = \varepsilon\int E_c E_c^* dV \qquad J_\omega = \frac{1}{2\pi}\int_0^{2\pi} Je^{-j\omega t}d\omega t$$

The field amplitude in the drive cavity

$$|a|^2 W_{EM} = P_{in}\frac{\omega}{Q_{ext}}\frac{1}{\left|\omega - \omega_c + \frac{i\omega}{2}\left(\frac{1}{Q_{ext}} + \frac{1}{Q_{losses}}\right) + \frac{I_b}{2aW_{EM}}\int d\xi\frac{c}{\omega}\left\langle\frac{v_\perp E_c e^{-i\omega t}}{v_z}\right\rangle\right|^2}$$

The total efficiency

$$\eta = \frac{\langle\gamma_i\rangle - \langle\gamma_f\rangle}{\langle\gamma_i\rangle - 1} = \frac{\gamma_0 + 1}{2\gamma_0}\frac{\alpha_0^2}{\alpha_0^2 + 1}\eta_\perp$$

From beam calculation

$$\eta_s P_{b,s} = \frac{\omega|a|^2 W_{EM}}{Q_s}$$

From fields calculation

Table 1 Design parameters of the electron gun.

Cathode-Anode Voltage	70 kV
Current	20A
Velocity Ratio	1.52
Axial Velocity Spread	12.5%
Beam Radius	2.6 mm
Magnetic Compression Ratio	6

Table 2 Gyroklystron microwave circuit parameters.

Cavity	Frequency(GHz)	Q factor	Mode
Input	34.20	80	TE_{021}
Buncher	34.05	50	TE_{021}
Penultimate	33.65	50	TE_{021}
Output	34.1	100	TE_{021}

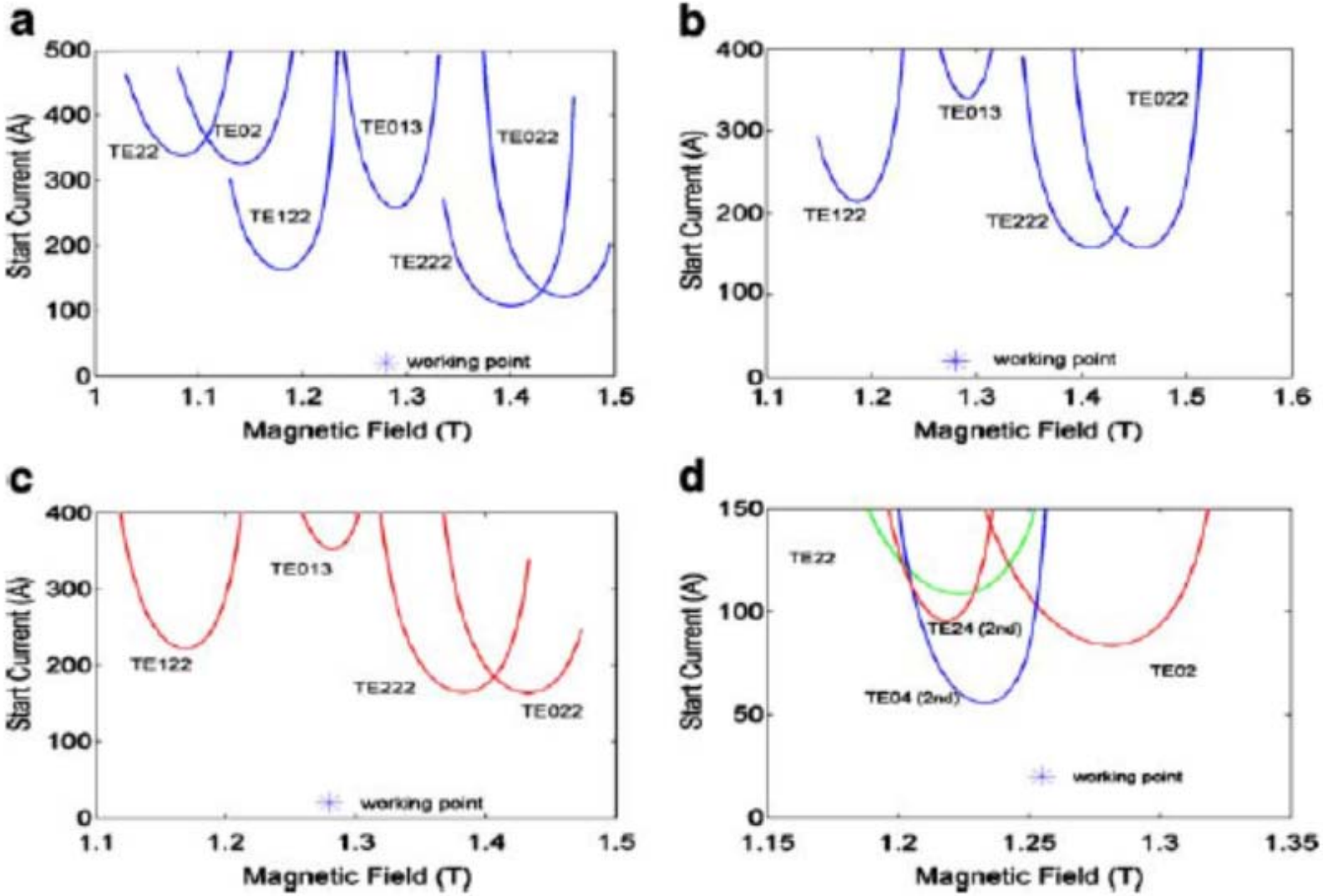

Fig. 3 Start current of the cavities: (**a**) input cavity, (**b**) buncher cavity, (**c**) penultimate cavity, (**d**) output cavity.

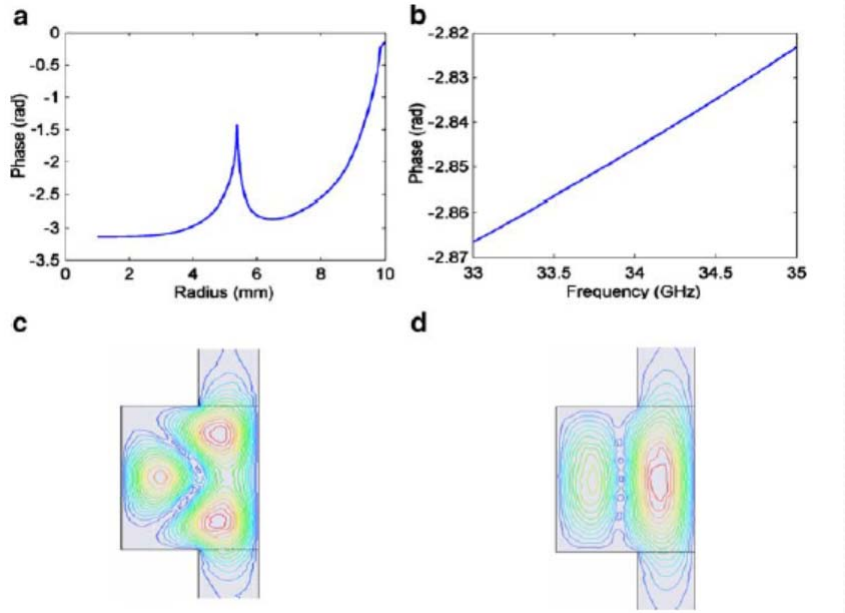

Fig. 4 (a) Dependence of 34 GHz TE01mode reflected phase on drift radius, (b) Dependence of TE01mode reflected phase on frequency, (c) The seriously effected TE021, (d) the perfect TE021 mode.

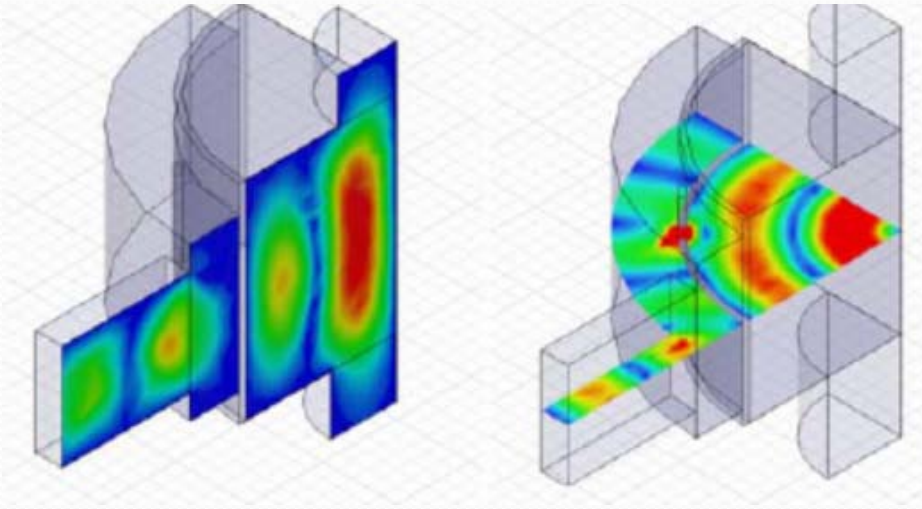

$$2\beta_{mn}L + \theta_L + \theta_R = N\pi$$

The input coupler: Power enters from the left into the coaxial resonator using a standard BJ320 waveguide. Then the power is coupled into the cavity though for coupling slots to establish the TE02 modes in the iner cavity

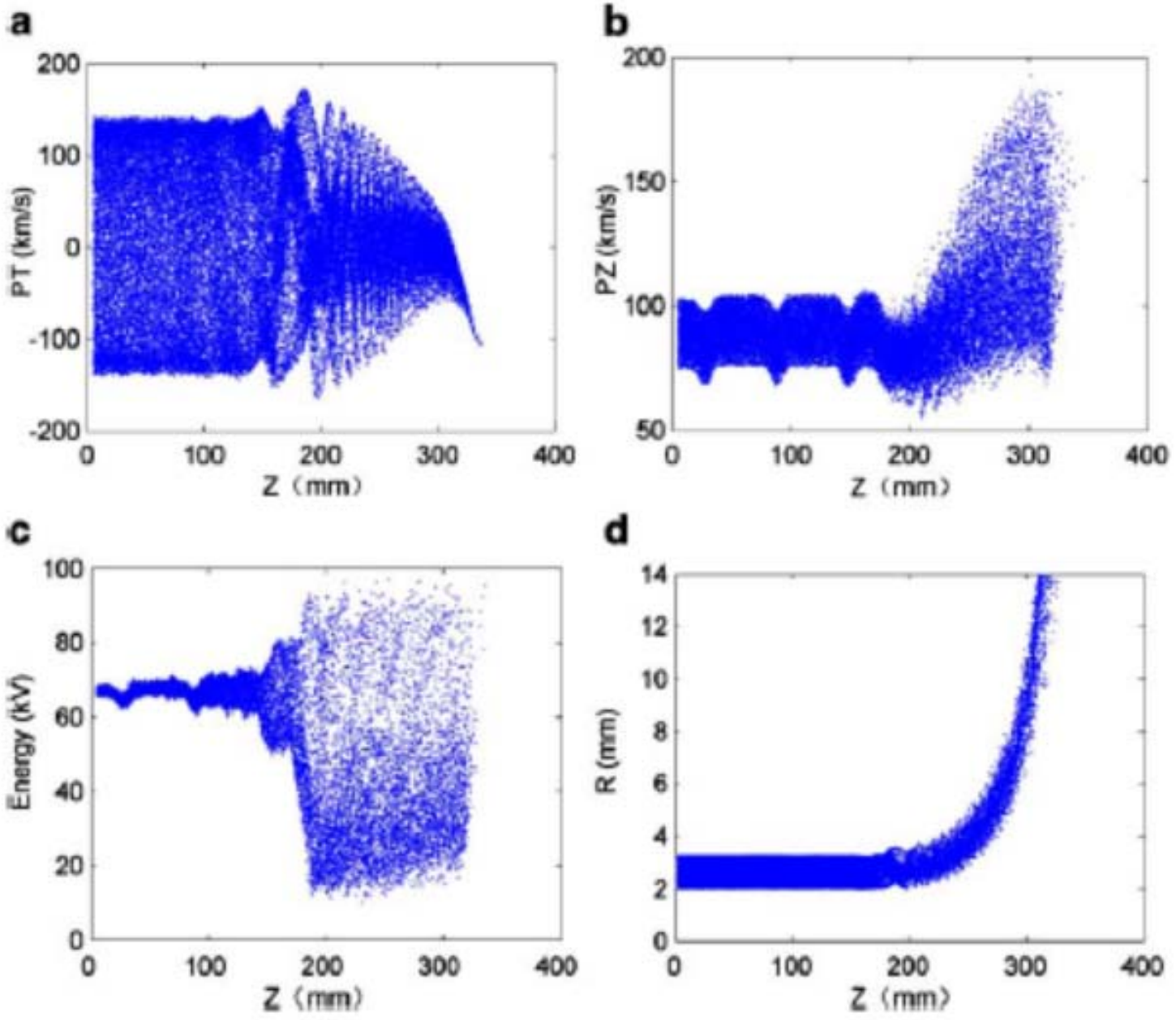

PIC simulation results.

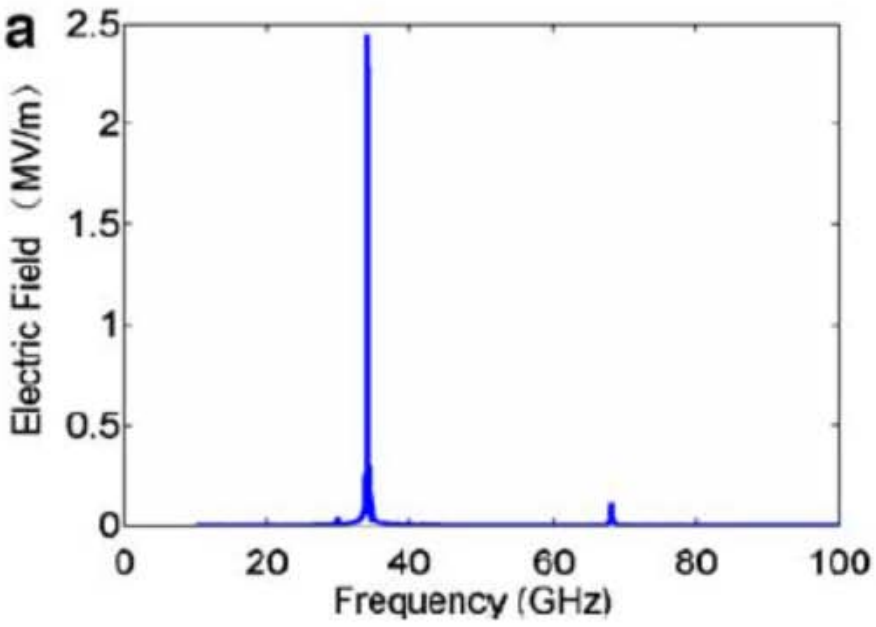

Frequency spectrum off the electric field

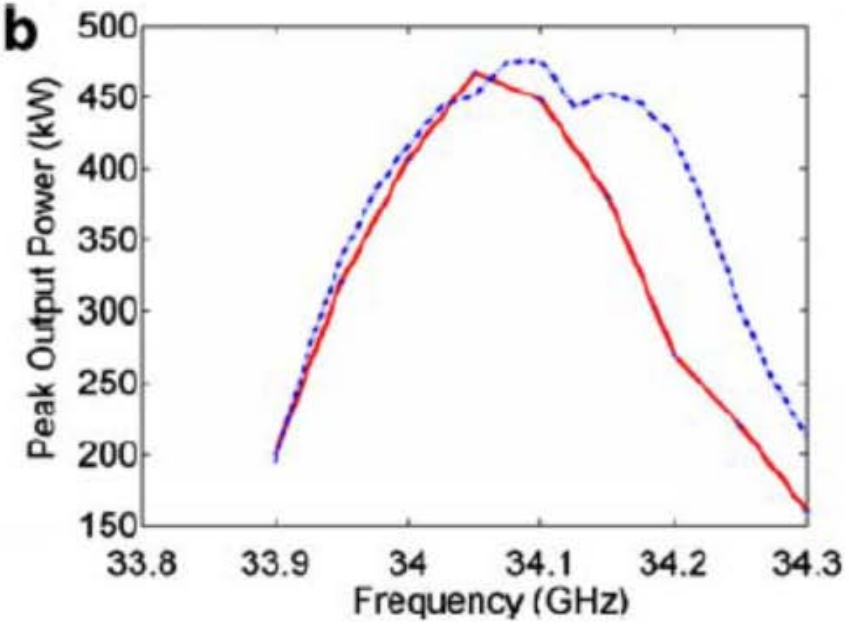

Dependence of output power on frequency by PIC(solid) and our nonlinear theory codes(dash).

More than 480kW output power, 34% efficiency. In the experiment, we got 400kW output power and 25% efficiency

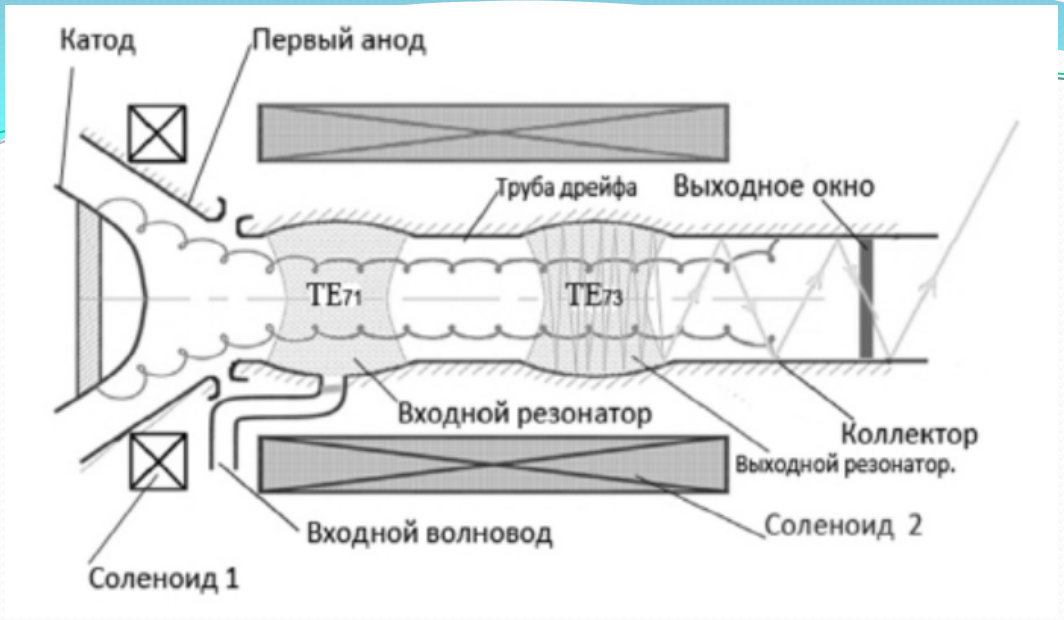

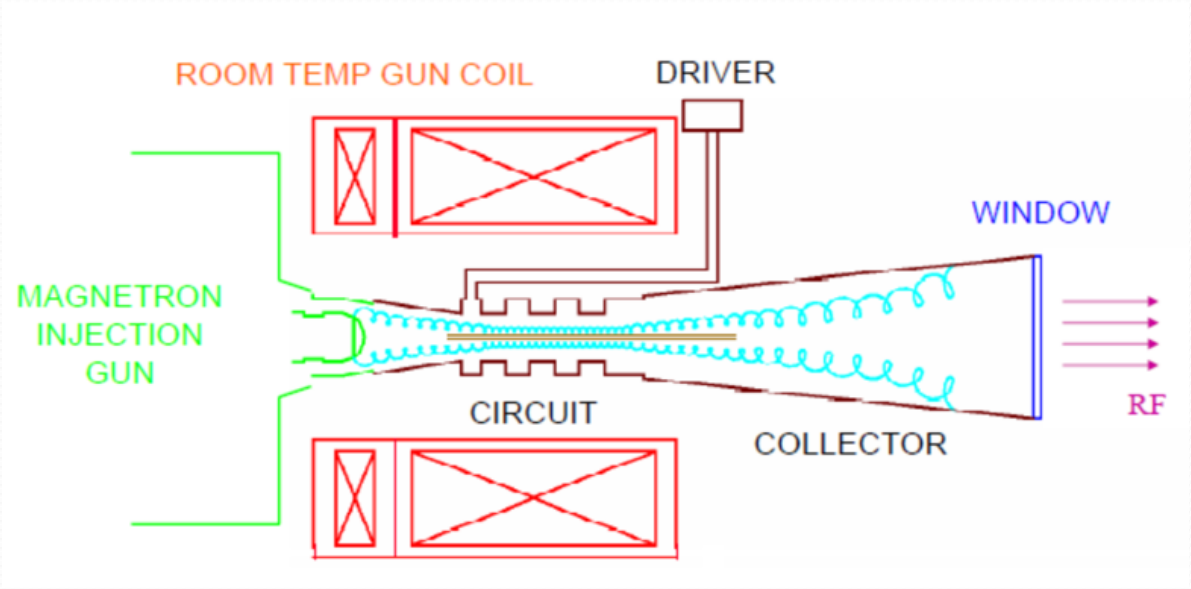

MW Gyroklystron Design

Thank You For Your Attention!